UNIVERSIDAD TECNICA
FEDERICO SANTA MARIA

Departamento de Obras Civiles

WIND-EFFECTS ON BAR-BUILT ESTUARY HYDRODYNAMICS

Memoria de Título presentada por

Dhannai Tamara Sepúlveda González

como requisito parcial para optar al título de la carrera de

Ingeniería Civil

y el grado de

Magíster en Ciencias de la Ingeniería Civil

Profesor Guía
Megan Elizabeth Williams

JANUARY, 2024

UNIVERSIDAD TECNICA
FEDERICO SANTA MARIA

TÍTULO DE LA TESIS:

WIND-EFFECTS ON A BAR-BUILT ESTUARY HYDRODYNAMICS

AUTOR:

DHANNAI TAMARA SEPÚLVEDA GONZÁLEZ

TRABAJO DE MEMORIA, presentado como requisito parcial para optar al grado de MAGÍSTER EN CIENCIAS DE LA INGENIERIA CIVIL de la Universidad Técnica Federico Santa María.

Nombre Profesor Guía: .....

Nombre Miembro 1 Comisión: .....

Nombre Miembro 2 Comisión: .....

Valparaíso, Chile, Enero, 2024

WIND-EFFECTS ON BAR-BUILT ESTUARY HYDRODYNAMICS

Dhannai Sepúlveda[1], Megan Williams[1]

1 Universidad Técnica Federico Santa María

Abstract

Although bar-built estuaries are widespread on Mediterranean coasts all around the world, including central Chile, little research has been undertaken on its closed state, when its system is transformed into a salty lagoon. Understanding the dependence of hydrodynamic response and thermohaline-stratification on strong wind events and its associated transport and mixing is of prime importance on the impact of water quality and eutrophication on ecosystems in coastal lagoons. In this study, we analyze the role of external factors such as wind velocities, freshwater flow, and wave overtopping in the hydrodynamics of a shallow, highly salt-stratified bar-built estuary. Vertical mixing and forcing currents, governed by wind surface stress, were quantified for diurnal and hourly time scales.

Data collected in early 2012 at Pescadero Estuary, California shows that in a close state there is a strong stratification and strong wind events during its closed state and due to its morphology wind is channelized into the along-estuary direction, causing the lagoon to receive mainly local forcing. Frequency spectral analysis is used to identify seiches on the surface due to upwelling caused by the wind. Wavelet analysis was also used to identify wave overtopping on the sand bar and observe the real effect of saline water entering the estuary. During strong wind events, buoyancy frequency was reduced to almost 0 from the 0.1 s^{-2} that the estuary usually had, and in some cases not return to its original value, showing upwelling and mixing of the water column. However, these effects varied over time depending on water level due to constant inflow from Pescadero and Butano creek. Some indicators like potential anomaly showed a good correlation with wind stress during the studied period. These preliminary findings show that wind effects are dominant in forcing vertical exchange of layers and generating currents at Pescadero.

Key words: bar-built estuaries, wind stress, stratification, upwelling, mixing

ACKNOWLEDGEMENTS (AGRADECIMIENTOS)

El buen término de este magíster se debe principalmente al apoyo económico de la Universidad Técnica Federico Santa María con su beca de arancel que cubrió completamente mis años de estudio en este programa y también al financiamiento entregado por ANID Fondecyt 11191077.

Quiero comenzar mis agradecimientos con las personas más importantes en mis años de estudios. A mi abuelita Georgina por siempre motivarme a dar lo mejor de mi y porque sin ella no estaría donde estoy, a mi mamá Sandra por ser mi apoyo emocional más fuerte y entregarme siempre su cariño, y a mi papá David por todos sus consejos de vida y por siempre contagiarme su alegría, quienes siempre estuvieron presentes en todo ámbito apoyándome con mi carrera y con mis proyectos personales. A mis amigas del alma que estuvieron presentes para los buenos y los malos momentos, con las que reí y lloré Karla y Francesca. A las amigas en las que siempre puedo confiar incondicionalmente y quienes siempre me van a escuchar y aconsejar, Daniela, Valentina, Ismaela y Paulina.

Agradecer igualmente a las personas que conocí en mi paso por la universidad partiendo por la profesora Megan, a quien agradezco por tomarme como estudiante, por todo lo que me enseñó en mis más de 2 años de Magíster y quien siempre me tuvo paciencia en lo que no entendía. A mis compañeros del equipo de Mecánica de Fluidos Ambiental con quienes tuvimos varias salidas a terreno y donde aprendí mucho. A quienes se volvieron como mi familia en los años de carrera, Claudio, Francisco y Mikel con quienes viví incontables aventuras en la época universitaria y en quienes siempre encontré apoyo en los momentos difíciles. Finalmente, agradecer a la persona que me ha acompañado por 7 años, aconsejandome, contagiándome su alegría y con quien las tardes y noches estudiando se volvieron más amenas. Gracias Bastian por apoyarme con mis metas y por ayudarme a ser la persona que soy hoy en día.

Contents

List of Figures

List of Tables

1 Introduction

Estuaries are geological formations that mark the interface between riverine and oceanic environments. These coastal waterbodies such as fjords, bar-built estuaries, and coastal lagoons are constantly exposed to anthropogenic or natural disturbances due to their productive importance (Schernewski, 2002; Martínez et al., 2007) and global changes (Winckler et al., 2020). These environments face challenges associated with rising sea levels, shifting precipitation regimes, and alterations in temperature patterns. Additionally, the coastal regions experience heightened human population growth, with a significant concentration of inhabitants residing near these areas (Neumann et al., 2015). This type of habitat is highly variable and dynamic and is where complex physical and biochemical processes take place.

Bar-Built estuaries are systems characterized by periodic/intermittently inlet closure through a sand bar (Whitfield and Bate, 2007). These are mainly found in Mediterranean climates such as Chile, California, South Africa, and Australia (McSweeney et al., 2017). Closure transpires when a barrier of sand accumulates within the entrance channel, leading to the obstruction of the passage. Such closures may manifest periodically based on seasonal variations or intermittently at irregular intervals throughout the year (Behrens et al., 2013). However, it is common that annual variability dominates closure events due to the marked seasonal cycles for rain and river flow observed in this type of climate (Ranasinghe and Pattiaratchi, 2003). Despite the variable nature of these systems, they are vital for many species that have adapted to take advantage of the closed-mouth condition (Viaroli et al., 2008).

When the estuary inlet closes, external factors like wind, river flow, and wave overtopping can impact its structure. This could be causing changes in the density due to fresh and saltwater input or surface stress by wind effects, causing upwelling, mixing, or circulation changing the estuarine ecosystem (Ranasinghe and Pattiaratchi, 1999). Wind stands as the predominant external force in play; however, the stratified nature of the system poses challenges in energizing the denser layer. Consequently, this often results in the suppression of turbulence beneath the pycnocline in certain instances (Cousins et al., 2010). The aforementioned makes these systems highly dynamic due to their variability in temperature and salinity, where intricate physical and biogeochemical interactions occur between oceanic and freshwater ecosystems. Species that inhabit these types of environments are vulnerable to conditions such as hypoxia or anoxia in the lower layers (Kelly et al., 2018) or the retention of nutrients in the bottom (Cousins et al., 2010) and when there is upwelling or mixing it could happen abrupt changes for marine life and generate them some problems or even death (Marti-Cardona et al., 2008).

Previous research has examined the impact of wind-induced shear stress on large thermal-stratified lakes, as demonstrated by studies conducted by Coman and Wells (2012), Laval et al. (2008), and Avalos Cueva et al. (2019). These studies have investigated the influence of wind stress, particularly in instances where they occur in timescales that are comparable to their natural oscillations. They have also identified the occurrence of upwelling events triggered by the wind, which in turn results in temperature variability. However, there is a dearth of information on the hydrodynamic effects of wind in smaller saline-stratified lagoons, and it would be interesting to explore this further to gain insights into the impact of wind on their behavior and structure.

This type of estuary is widely spread in Chile's Mediterranean regions, which seasonal conditions are similar to those of other places, already mentioned, where they are found, and despite this, there are few studies carried out in the country on the subject. In Dussaillant et al. (2009) an investigation was carried out on the Yali reserve, one of the most important wetlands in the central zone of Chile, whose knowledge must be

complemented to fully understand the small bar-built coastal systems.

1.1 The Pescadero estuary

Pescadero Estuary is a small and highly stratified bar-built estuary situated at the convergence of Pescadero Creek and Butano Creek on the California coast. It is located 60 [km] south of San Francisco Bay and 40 [km] north of Monterrey Bay (Fig. 1). The hydroclimate of Pescadero in the Mediterranean region exhibits an average yearly precipitation of 750 [mm]. This area experiences a distinct wet season, notably cooler, spanning from November to April, followed by a warmer and drier season extending from May to October (Largier et al., 2015). The hydrodynamic phenomena observed in Pescadero demonstrate similarities to those witnessed in analogous estuarine systems along the western coast of the Americas, Australia, and South Africa. Moreover, resemblances are evident in estuaries situated within Mediterranean climates on the Atlantic western coast of Europe, along with shallow coastal waterbodies with a sand bar found in various other locations.

Figure 1: Location of Pescadero Estuary on California's Coastline. Images reprocessed from Google Earth.

The sand barrier placed at the inlet of Pescadero closes the estuary from the sea, changing its behavior to a stratified lagoon which usually happens during the dry summer season (Williams, 2014). Inlet rupture usually occurs during the wet season when precipitation increases flow and the lagoon fills to overflowing. Consequently, this overflow leads to the formation of a fresh channel between the lagoon and the resumption of tidal influence, allowing seawater to infiltrate the estuary once again (Largier et al., 2015). During periods when the mouth of the estuary is closed, the water level of the lagoon rises and could flood the surrounding marshy land.

This site holds significant importance due to several factors. Firstly, the detection of fish kills subsequent to the breach of the lagoon mouth following an extended closure, as identified in the research conducted by Largier et al. (2015). Additionally, the surrounding agricultural lands hold significant productive value for the local community. However, the area also presents a few concerns, such as the risk of winter flooding in low-lying lands, which includes some roads and parts of the town. Another factor is the presence of a wide diversity of habitats and microhabitats in the estuary, which require careful monitoring and management to preserve their ecological balance.

Pescadero has two main water inputs: freshwater inflow and saline water, which sometimes get mixed and other times form a two-layer structure. The behavior of the estuary depends on the mouth state, where we can observe an 'open' and 'closed' state. Pescadero receives freshwater inflow from two relatively small watersheds, which have fluctuating discharges that exhibit high variability, influenced by daily fluctuations in precipitation during the wet season, as well as seasonal and annual variations (Largier et al., 2015). The Pescadero watershed encompasses approximately double the area of the Butano watershed, and produces 57% of the streamflow (Williams, 2014). The coastal region of Northern California encounters a semidiurnal tide pattern characterized by a neap tide range of less than 1 m and a spring tide range reaching nearly 3 m (Williams, 2014). Saltwater get into the estuary easily during open state, but when the inlet is closed seawater has to overtop the sandbar to get into the estuary, which happens occasionally during high tide and strong waves.

1.2 Motivation

In its state of disconnection from the ocean (i.e., closed state), a bar-built estuary can take the form of a shallow stratified lagoon, due to the presence of saltwater and freshwater from fluvial inputs (Behrens et al., 2016). This estuary state could lead to eutrophication if there are no energy inputs to the system (Nunes and Adams, 2014), and usually, the wind is the main source, driving to mixing and destratification in small bar-built estuaries (Gale et al., 2006) triggering processes that impact mixing and circulation, which could affect the marine life of the estuary (Marti-Cardona et al., 2008).

In cases where stratification is strong, it can create a barrier, known as the pycnocline, between the denser and lighter layers of water. This pycnocline acts as a barrier that suppresses turbulence and mixing below it, making it difficult to energize and mix the denser layer with the lighter layer. As a result, the denser layer remains stratified and separated from the lighter layer, leading to a lack of vertical mixing and exchange between the layers (Cousins et al., 2010). This phenomenon can occur in various water bodies, including estuaries, lakes, and oceans, and has implications for the distribution of nutrients, oxygen (Kelly et al., 2018), and other properties within the water column, which can impact the overall ecosystem dynamics and health of the water body (Marti-Cardona et al., 2008).

These waterbodies are highly dynamic, so it is crucial to understand the mixing and stratification dynamics of aquatic systems. Estuaries are the connection between the earth and the ocean, receiving waters coming from rivers and creeks that are exposed to anthropogenic effects, causing changes in freshwater flow or temperature, in addition, to being subjected to sea level rise and wave climate variations (Winckler et al., 2020; Holt et al., 2010; Thorne et al., 2021). Besides, in the estuaries, of their contact with the coast and rivers, activities such as fish farming or agriculture are developed, so they have economic and social importance to communities.

The upwelling effect caused by wind forcing has potential relevance in nutrient and oxygen exchange between layers (Kelly et al., 2018) and has been studied widely in lakes using temperature measurements (Coman and Wells, 2012; de la Fuente et al., 2010; Roberts et al., 2021), however, there are fewer studies that observe this kind of behavior at bar-built estuaries or in smaller coastal lagoons.

Previous studies in this estuary have included mesoscale system behavior and trajectory revealing disturbance-response-recovery regimes of the sandbar (Clarke et al., 2014), also including fish habitat studies considering fish behavior and changes in water quality (Huber and Carlson, 2020) due to opening or closing of the sandbar (Richards et al., 2018). In addition, to studies about tidal stress and how it discontinuously affects the estuary due to mouth restriction (Williams and Stacey, 2016).

Our study seeks to study the hydrodynamic behavior of Pescadero when it is in its closed state in order to quantify the effects of external factors such as wind, freshwater flow and the effect of the tide. Given the existing literature in other estuaries similar to Pescadero, it is expected that wind shear stress at the surface is the major cause of upwelling and mixing. In addition, the entry of freshwater into the estuary together with the fortuitous entry of seawater due to wave overtopping is expected to generate a density gradient that has an effect on stratification, as opposed to the effects of wind that de-stratifies, but not before the tidal and freshwater currents generate a shear stress at the surface. A water level analysis will also be performed where wind and waves overtopping the sand bar are expected to generate surface fluctuations.

2 Objectives

2.1 General objective

The main goal of the present work is to comprehensively understand and quantify the drivers of stratification and mixing in closed bar-built estuaries. These estuaries are characterized by a mouth that is periodically closed by sandbars, leading to unique hydrodynamic conditions. By investigating and analyzing the factors that influence stratification and mixing in such estuarine systems, this research aims to provide insights into the physical processes that govern water column structure and dynamics in these environments. The findings of this study will contribute to a deeper understanding of how external forces, such as wind stress, freshwater input, and wave overtopping, interact with the complex estuarine morphology to influence stratification and mixing patterns. This knowledge will have practical implications for the management and conservation of closed bar-built estuaries, as it can inform decision-making related to water quality, ecosystem health, and coastal resource management. Our focus of investigation involves the Pescadero Estuary, an exemplar of bar-built estuaries situated in California, exhibiting similarities to numerous other small inlet systems found across Mediterranean climates globally.

2.2 Specific objectives

The specific objectives of this study are:

(1) To investigate the velocity and density variability in a small, highly stratified estuary during its closed state. The findings will contribute to our understanding of water column dynamics in closed bar-built estuaries.

(2) To identify the influence of wind stress on the hydrodynamics of a closed bar-built estuary. This research will contribute to a better understanding of the relationship between wind stress and estuarine stratification.

(3) To study the wind-estuary interaction and the effects of other external factors such as water inflow and wave overtopping. This is crucial for understanding the dynamics of estuarine stratification and mixing, which have significant implications for water quality, ecosystem health, and resource management.

3 Literature review

3.1 Bar-built estuaries in the ecosystem and the community

Climate change is affecting multiple marine ecosystems globally (Hewitt et al., 2016). It has been observed that the overall oxygen content in the global oceans has declined over the past five decades (Schmidtko et al., 2017) and that air temperature is increasing in oceans (Omstedt et al., 2004; Jones et al., 1999). Some studies expect that the absolute mean sea level on Chilean coasts rises between 0.35 to 0.74 m in the next 80 years (Winckler Grez et al., 2020). The effects of climate change can put at risk the coastal zones, including estuaries and coastal lagoons which are especially abundant ecosystems in flora and fauna.

In addition, there is evidence that there is a decrease in surface wind speeds in Northern Europe (Woolway et al., 2017) and an increase in along-shore winds in the Chilean coastal zone (Winckler Grez et al., 2020). It is known that changes in surface wind speed affect the number of days that a lake is stratified, which affects the nutrient availability and quality of a waterbody, changing the amount of oxygen present in deep waters (Woolway et al., 2017). It is important to study wind effects in estuaries to be able to quantify how wind-speed changes will affect these environments.

In central Chile, there is a decrease in river discharges affecting buoyancy and stratification (Winckler Grez et al., 2020), which can be causing a wide range of changes in estuarine and marine ecosystems, including changes in oxygen availability. These changes can impact fish populations and other autotrophic organisms.

The importance of intermittently closed estuaries goes beyond local impacts. These estuaries can accumulate sediment while the inlet is closed (Thorne et al., 2021), and in rainy seasons they open their mouth naturally because of the increase in freshwater inflow (Hoeksema et al., 2018). This process settles sediments to the nearby marshes helping to maintain their elevation according to the sea level, mitigating the consequences of sea level rise (Thorne et al., 2021). The mouth, maybe, is exposed to artificial openings to avoid flooding the surrounding lands (Behrens et al., 2013), which does not allow the sediments to set in the marsh platform (Thorne et al., 2021), not allowing them to keep their normal elevation that protects the coastal zone from the sea level.

Increased river discharge due to climate change could lead to increase erosion and the number of suspended particles of sediment in the water (Whitfield and Wooldridge, 1994). Enhanced sediment concentration could lead to accumulation in the estuary, changing the equilibrium of opened and closed state of the sand bar, which along with the increase of freshwater input could flood the surrounding land, and decreased discharge could do the opposite (Peeters and Kipfer, 2009). Consequently, depending on the vegetation present and its oxygen demand, deep-water oxygen may be reduced or suppressed (Kelly et al., 2018; Largier, 2021). Also, the density of the surface waters will be reduced and thus could change the estuary behavior to external

factors such as wind stress.

Bar-built estuaries are under continuous anthropogenic stress due to their closeness to human settlements (Clark and O'Connor, 2019) and their productive importance. Dams constructed upstream for water storage reduce the freshwater that goes to the ocean, causing the retention of suspended sediments. This results in a change in the morphology of the estuary due to not receiving the sediments that used to accumulate in the inlet, leading to premature scour of the sand bar (Peeters and Kipfer, 2009). Also, to prevent flooding of roads or agricultural lands nearby, the community plan the opening of the inlet artificially, which could result on abrupt changes on the estuary ecosystem Behrens et al. (2013).

3.2 How bar-built estuaries are studied in Chile and around the world

McSweeney et al. (2017) studied the bar-built estuaries all around the world and their climatic, marine, and fluvial conditions to classify them and quantify the drivers of their distribution in each continent. That let the estuary response to climate change and human impacts to be estimative and include integrated coastal managment, reducing impact in the environment.

Dussaillant et al. (2009) studied a Chilean coastal lagoon in its open and closed state and observed that in its closed state the rainfall influence was not important except for the storms that open the inlet to the sea. He also observed that wind effects can be important during the disconnected phase to the ocean, producing a slope in the lagoon levels. He studied the connected phase using a general pattern, spectral, and Fourier analysis.

In their study, Gale et al. (2006) investigated the dynamics of Intermittently Closed and Open Lakes and Lagoons (ICOLLs) during their closed state. The research findings revealed that the presence of stratification can lead to depletion of oxygen in the bottom waters. This particular factor has been associated with fish kills in Pescadero, as documented by (Largier et al., 2015).

Kelly et al. (2018) conducted a study on Lough Furnace, Ireland, a naturally deep saline lagoon characterized by restricted tidal inflows and long periods of low freshwater input, which showed continuous vertical stratification and anoxia in the lower layers. The study found that specific tidal events and wind-driven upwelling could oxygenate the deeper layers, revealing a correlation between tidal influence and wind stress in vertical mixing.

Behrens et al. (2016) observed the salt intrusion in a bar-built estuary and its differences between closed and open state conditions. The research identified the existence of interchanging shallow sills and deep pools within the estuary. These formations function to confine the saltwater subsequent to its intrusion into the estuary. The study proposed that internal seiche motions occurring in the outer estuary trigger the intrusion process. These motions lift saline water within the pycnocline to a height adequate for cresting the sills. During the estuary's closed state, this intrusion of salinity spans distances of several kilometers away from the shoreline.

In Rodeo Lagoon, a shallow strongly-stratified lagoon, (Cousins et al., 2010) investigated the effect of stratification on water column parameters such as salinity, dissolved oxygen, and nutrient levels. They found that stratification causes a significant suppression of turbulence below the pycnocline, resulting in the confinement of nutrients in the lower layer for several months. The study revealed that wind is the primary source of

mixing in the lagoon, and destratification by wind facilitates the redistribution of nutrients from the lower brackish layer.

3.3 Hydrodynamics of a stratified waterbody

In nature, stratified waterbodies can be found not only in estuaries (Human et al., 2016) but also in lakes (Valerio et al., 2012; Imam et al., 2013; Coman and Wells, 2012), coastal lagoons (Cousins et al., 2010) and also in oceans: continental shelf seas, river plumes, etc. Although lakes are usually studied as thermally stratified water systems, they exhibit comparable hydrodynamics to thermal-haline stratified coastal waterbodies. In estuaries, when the tidal connection with the ocean is limited, water circulation is driven by wind and freshwater inflow, resulting in similar dynamics to lakes in a smaller scale.

The lake or estuary may exhibit an upwelling response contingent upon the intensity and duration of wind forcing (Shintani et al., 2010). Upwelling is a significant process that occurs in stratified estuaries and lakes, influencing their hydrodynamics and ecosystem dynamics. It involves the vertical transport of nutrient-rich, deep oceanic waters to the surface, promoting enhanced biological productivity and supporting diverse marine ecosystems (Gupta et al., 2022).

One parameter commonly used to characterize upwelling in estuaries is the Wedderburn number (Imberger and Hamblin, 1982). The Wedderburn number (W) is a dimensionless parameter used to quantify the relative importance of wind stress to stratification in a water column (Patterson et al., 1984). It characterizes the balance between the energy from wind forcing and the energy required to mix the upper layer with the lower layer in stratified systems (Monismith et al., 2006a). A high W indicates that wind stress is dominant and can overcome stratification, promoting mixing, while a low W suggests that stratification is dominant, inhibiting mixing. Researchers use W to assess the impact of wind on the vertical structure and circulation of water in stratified environments (de la Fuente et al., 2008; Wüest and Lorke, 2003). By quantifying the Wedderburn number, researchers can assess the strength and effectiveness of upwelling processes in bar-built estuaries, aiding in the understanding and management of these dynamic coastal environments.

The wind's energy is the primary source of energy for the water column's circulation, and it can cause an upwelling response when it is strong enough to overcome the stratification of the water layers. Upwelling occurs when the wind's energy forces the lower layer of water to move upward, bringing nutrients and other materials to the surface that can stimulate primary productivity in the water column (MacIntyre et al., 2010).

Roberts et al. (2021) studied the setup and relaxation of spring upwelling in a deep, rotationally influenced lake, Lake Tahoe, using a combination of field observations and numerical modeling to investigate the mechanisms that cause the upwelling of deep water in the lake. They found that the setup of upwelling was a wind-induced barotropic effect, that was dependent of wind duration and bathymetry. The relaxation of upwelling occurred when the wind stopped, and the potential energy was converted into kinetic energy, which led to the downwelling of surface water. These findings provide new insights into the mechanisms that control the dynamics of upwelling in deep lakes and could help inform the management of these ecosystems.

The Wedderburn number was design for rectangular basins, but this approach is not too close to reality, where basins can be of multiple and irregular shapes. Shintani et al. (2010) used a numerical model to demonstrate that the upwelling of deep water in lakes with any geometry can be described using the Wedderburn number as a function of the Richardson number, the buoyancy frequency, and the Rossby number. The Wedderburn

number offers a broad estimate of interface behavior, serving as a scale for seiching phenomena without providing intricate details. These results provide a better understanding of the physical processes that drive the upwelling of deep water in lakes and could help improve the management of these ecosystems.

Wind stress also induces a tilting of at the interface between layers of different densities (Monismith, 1985). This inclination of the interface leads to the transmission of momentum from the wind to the water column. This interface tilt results in the transfer of momentum from the wind to the water column, leading to mixing and vertical exchange processes.

Monismith (1985) discussed that a three-layered fluid has a similar behavior as a two-layered fluid when the upper layer is shallow. This is because the shallow upper layer behaves like a mixed layer, while the middle layer acts as an interface layer separating the mixed layer from the lower layer. When the upper layer accelerates due to a wind forcing in the surface, the mixed layer starts to deepen rapidly, while the upper layer tilts and might upwell (Monismith et al., 2006b).

The response of stratified lakes or estuaries to wind forcing events can be complex, involving interactions between the layers of the water column, upwelling responses, and changes in the water column's stability (Jayaweera et al., 2019). Upwelling occurs when the wind's energy forces the lower layer of water to move upward, bringing nutrients and other materials to the surface that can stimulate primary productivity in the water column (Bastidas et al., 2021). The thickness of the interface layer is an important parameter that can impact the dynamics of the water column in these types of waterbodies (Xu et al., 2017). Factors such as wind strength and duration, water temperature, and the presence of nutrient-rich layers in the water column can all affect the response of stratified lakes or estuaries to wind forcing events (Nidheesh et al., 2018).

Estuarine ecosystems are profoundly influenced by freshwater inflow, which shapes their dynamics through the mechanism of estuarine circulation. The interplay between freshwater and seawater establishes horizontal density gradients, initiating the circulation process. This involves the movement of lighter surface water seaward over denser water moving landward below. The importance of freshwater-induced circulation in estuaries is widely acknowledged in the literature, particularly emphasized by Simpson et al. (1985). His work highlights the fundamental role of freshwater inflow in generating horizontal gradients that propel estuarine circulation, thereby influencing the overall dynamics of these ecosystems.

Simpson et al. (1985) research explores the intricate relationship between tidal processes and stratification dynamics in estuarine systems. He demonstrates that the density gradient interacts directly with the vertical shear stress of the tidal stream, contributing to periodic stratification. This periodicity exhibits temporal variations, with a positive effect during the ebb phase of the tide. Additionally, Simpson introduces the concept of tidal deformation affecting the horizontal density gradient, leading to variations in stability during different tidal phases. The balance between these stratifying mechanisms and tidal stirring, opposing them, plays a crucial role in determining the enduring and periodic nature of stratification in estuarine waters.

Building on these findings, Simpson et al. (1991) expands the scope of investigation to consider the broader factors influencing water column stability in estuaries. His work highlights the significance of estuarine circulation, driven by horizontal density gradients, as a primary process controlling water column stability. Furthermore, the study incorporates the role of mixing induced by both tidal and wind stress, along with the deformation of the density field caused by tidal shear stress. This comprehensive perspective underscores the multifaceted nature of factors influencing stratification in estuarine environments, providing valuable insights for a deeper understanding of these complex ecosystems.

3.4 Pescadero estuary studies

Recent studies on the Pescadero Estuary have focused on fish kills that occur when the sandbar closes, leading to the creation of an anaerobic environment in the bottom waters (Sloan, 2006). Geochemical analysis of sediments has shown that the shift from a closed to an open state results in adverse water conditions within the Pescadero Estuary, marked by numerous indicators surpassing optimal values for fish and aquatic life (Richards et al., 2018). Huber and Carlson (2020) documented one of the breach-induced fish kills events, illustrating an instance of compromised ecosystem function due to persistent deterioration in water quality during the closed estuarine phase. While previous literature on the Pescadero Estuary has focused on management plans for biological productivity (Curry et al., 1985) or preserving the hydrology of the estuary (Williams et al., 1990), these recent studies highlight the importance of understanding the physical and chemical dynamics of bar-built estuaries.

In addition to the effects of sandbar closure, physical phenomena such as the effects of the constriction generated by the mouth in its open state have been studied. Williams and Stacey (2016) observed that wave setup and tides regulate the water level in the estuary, while the sandbar at the mouth restricts ocean gravity waves' access but allows infragravity motions to traverse the inlet. This mechanism induces significant energetic velocities. These investigations underscore the profound reliance of small bar-built estuaries on nearshore processes, and the need to understand the complex interactions between external factors and estuary dynamics.

4 Methods

4.1 Field measurements

Four field campaigns were carried out between 2010 and 2012 described in the work of Williams (2014) and Williams and Stacey (2016). This work focus exclusively on the data between January and March 2012 to analyze the behavior of the estuary in a closed state. Measurements were made in the estuary using instruments for velocity and depth, as well as a meteorological station to collect wind speed and direction data in the marsh.

Depth data were collected using moored Conductivity, Temperature, Depth sensors (RBR XR-420 CTD) placed at different heights and distributed along the estuary at four locations as shown in Fig. 2: Near Mouth (NM), Mid-Lagoon (ML), Deep Channel (DC), and Pescadero Creek (PC). It should be noted that the instruments placed along the water column are floating, so they have range of motion in the vertical (Fig. 3). The estimated difference in the instruments depth between DC and the others is of 0.8 m for NM, 0.75 m for ML and 0.7 for PC. We have to consider that the instruments PC and NM were moved in 16 Feb., so we estimated the value after that day. Density profiles were made on 16 Feb. with a CTD logger around 5 p.m. at the locations indicated in Fig. 2.

Velocity measurements were made with an Acoustic Doppler Current Profiler (ADCP 1200 KHz WH) anchored to the bottom of the estuary at location DC. This instrument is designed to be used in deeper water, so data collected from the surface could be affected by the interference caused by reflection. Also, this instrument, despite it is on the location DC, does not have the same depth than the CTD moored at the same location, due to the bathymetry (See diagram of Fig. 2).

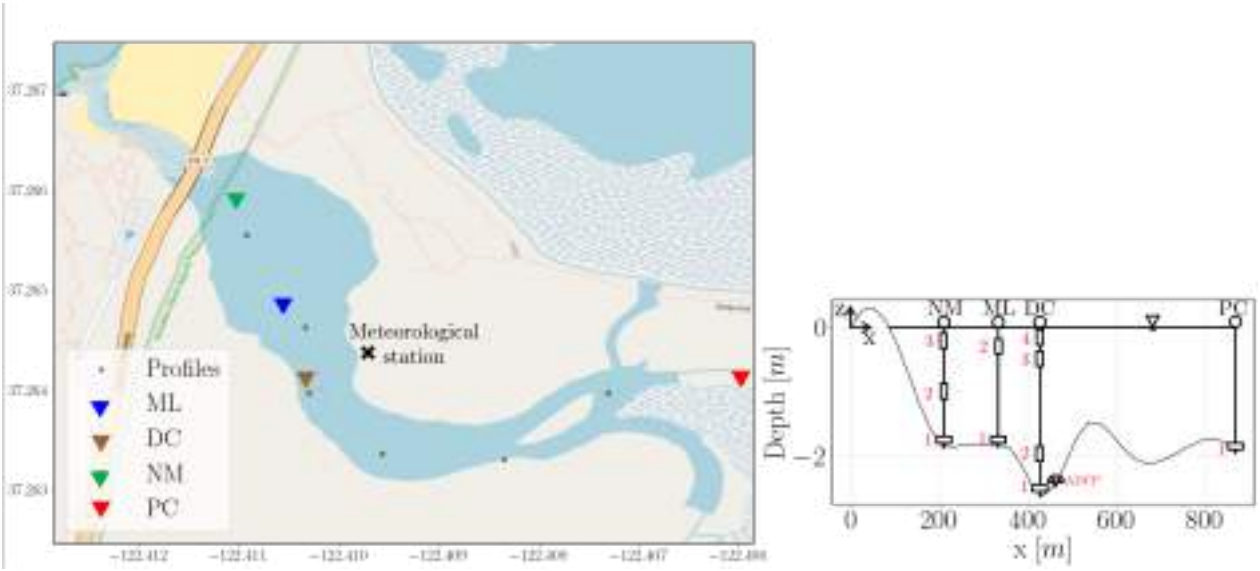

Figure 2: Pescadero estuary map and location of the moorings (NM: Near Mouth, ML: Mid-Lagoon, DC: Deep Channel and, PC: Pescadero Creek), meteorological station. Profile locations for CTD measurements in Fig. 2 are indicated by small "x". Diagram of the elevation view of Pescadero in the along-estuary direction with the locations of the sensors in the water column.

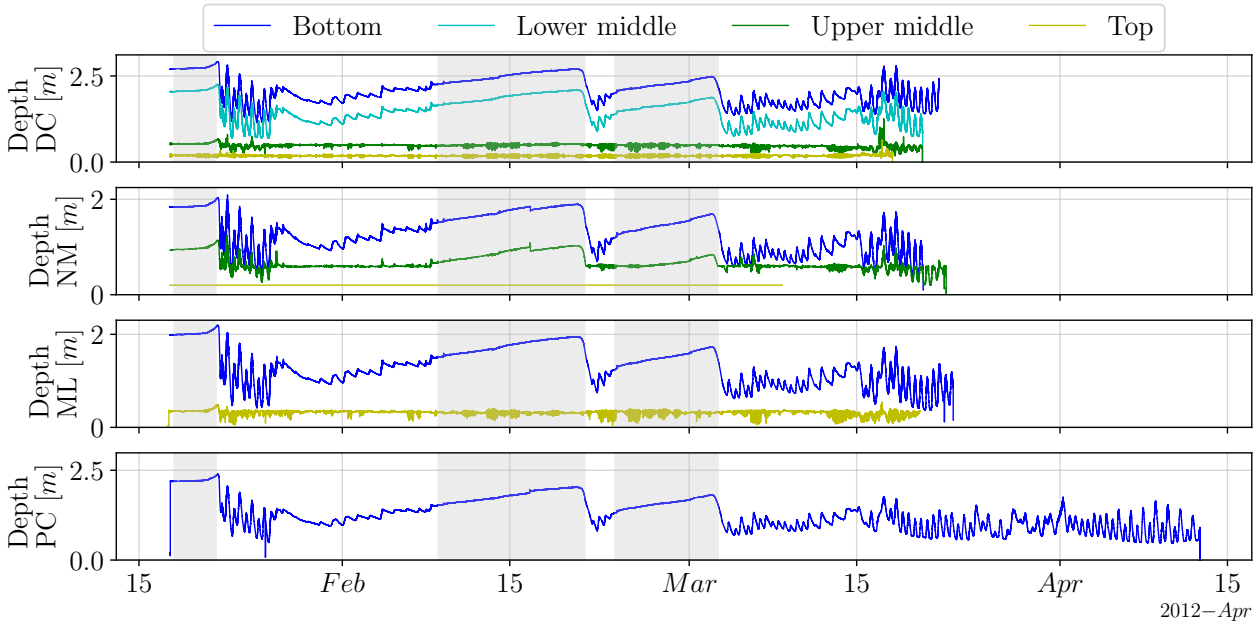

Figure 3: Time-series of instruments depth in all locations. The windowed data is the used in this study.

For wind speed data, an anemometer (Model #05106, RM Young Fig. 4) was installed at a height of 3 meters above the water surface within marshy land bordering the estuary (Fig. 2). All the information of the instruments are summarized in Table 1.

Figure 4: Anemometer for wind measurements. Model #05106, RM Young. (Williams, 2014)

Table 1: Information of the instruments used in the field campaign.

Location		Instrument	Sampling Rate	Height above bed	Dates of data
NM	1	RBR XR-420 CTD	10 s	0 cm	17/01/2012 - 20/03/2012
	2	RBR XR-420 CTD	30 s	50 cm - 90 cm	17/01/2012 - 22/03/2012
	3	RBR XR-420 CTD	30 s	75 cm - 1.7 m	17/01/2012 - 08/03/2012
DC	1	RBR XR-420 CTD	10 s	0 cm	17/01/2012 - 21/03/2012
	2	RBR XR-420 CTD	10 s	50 cm - 80 cm	17/01/2012 - 20/03/2012
	3	RBR XR-420 CTD	10 s	1 m - 2 m	17/01/2012 - 20/03/2012
	4	RBR XR-420 CTD	10 s	1.3 m - 2.6 m	17/01/2012 - 18/03/2012
	1	ADCP	2 Hz	0 m	16/02/2012 - 14/03/2012
ML	1	RBR XR-420 CTD	10 s	0 cm	17/01/2012 - 20/03/2012
	2	RBR XR-420 CTD	10 s	40 cm - 1.6 m	17/01/2012 - 23/03/2012
PC	1	RBR XR-420 CTD	30 s	0 cm	17/01/2012 - 12/04/2012
Profiles		RBR XR-620 CTD	6 Hz	-	16/02/2012
Met. station		Model # 05106, RM Young	6 min	-	27/10/2011 - 19/04/2012

4.2 External data

To supplement the data, the estimation of freshwater streamflow entering the Pescadero estuary relies on readings from a gauge operated by the United States Geological Survey (USGS) positioned on Pescadero Creek approximately 8.5 kilometers upstream from the estuary's mouth (USGS 11162500). As the Butano creek is also contributing, the total discharge estimation given by Williams (2014) is $Q_T = 1.76Q_{P,C}$ to account for the watershed area downstream of the gauge.

The tide height data in San Francisco Bay and Monterrey Bay (stations 9414290 and 9413450 respectively) were obtained from the National Oceanographic and Atmospheric Administration (NOAA). Wave climate data were obtained from the National Data Buoy Center, 40 km offshore from the coast of Half Moon Bay (station 46012) (Fig. 5).

Figure 5: Stations and sites locations of the external data obtained for this study.

4.3 Data processing

4.3.1 Salinity and temperature

The CTDs measurements were made with a frequency of 10 or 30 sec, and at each location, there were one (PC), two (ML), three (NM), or four (DC) instruments at different depths (Table 1). The bottom pressure measurements at each sensor were corrected for sea-level atmospheric pressure measured at the nearest weather station located at the Half Moon Bay airport. This work focuses exclusively on the two periods where the estuary is closed between February and March.

We subjected the data to quality control, where data from the beginning and end, when the instrument was out of the water, and some data in the middle, where we observed time jumps incompatible with reality, were eliminated. Density is calculated from salinity, temperature, and pressure data, by the GSW Python package which is an implementation of the Thermodynamic Equation of Seawater (TEOS-2010) (Roquet et al., 2015).

Additionally, CTD profiles were made on 16 Feb., between 17:00 and 17:30 which were used to calculate the density also using TEOS-2010. When the profiles were taken the wind was very calm so we can say that the estuary was not having any significant external forcing.

4.3.2 Water velocity

Velocity data collected with the ADCP in its raw form is composed of different points measured throughout the water column (bin), which were in instrument coordinates. Some of this bins were measured out of the water.

First, we removed the bins above the surface from the record and then rotated them to earth coordinates (East, North) using the method shown in Teledyne (2008).The ADCP has a blank space of measures at the bottom, so the first measured point was 71 cm above the ground, meaning there is only a window of velocity data in the water column (Fig. 6).

The velocity data obtained from the ADCP, considering all bins that were not deleted, was processed using an axis-rotation technique to align the measurements with the principal coordinates (u, v). This transformation was performed based on the direction of maximum variance, as illustrated in Fig. 7. The data analysis covered

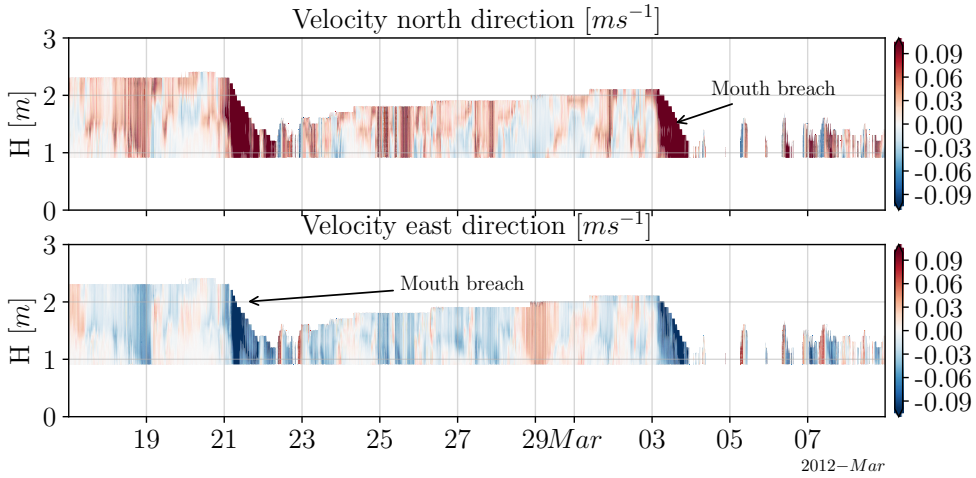

Figure 6: Timeseries of velocity data plotted in North and East directions in the water column.

the period from 17 February to 9 March, which encompassed two observed breaches of the estuary mouth, as depicted in Fig. 6. The inclusion of these inlet openings was essential to capture the inflow direction during estuary draining events. The principal direction angle was determined to be 48.6° clockwise from the west axis, and it was established that the positive velocity component (u) corresponded to the flow direction towards the sea.

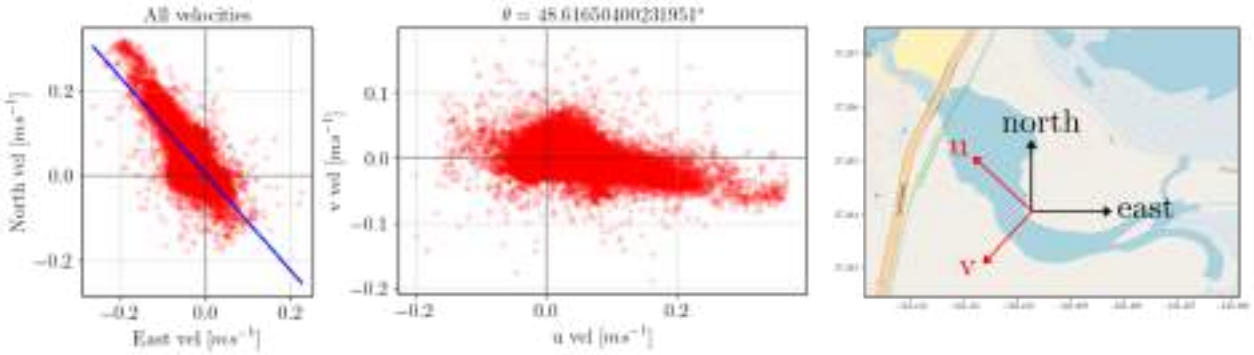

Figure 7: Velocity data plotted in North-East and $u - v$ coordinates, and a map of Pescadero signaling the coordinates.

Fig. 2 shows that the ADCP instrument and de CTD instrument in DC were not at the same depth due to bathymetry. To level both instruments to a common coordinate system we estimated the difference in depth using the location of surface that both instruments had. We adjusted the first cell of the ADCP to 0.91 m above the bottom of the estuary.

4.3.3 Wind velocity

Raw wind data contained the velocity magnitude and direction as shown in Fig. 8. Wind velocity coordinates were transformed first in east-north coordinates. Then, the data were also axis-rotated to the principal coordinates of the estuary currents, with an angle of 48.6^{o}.

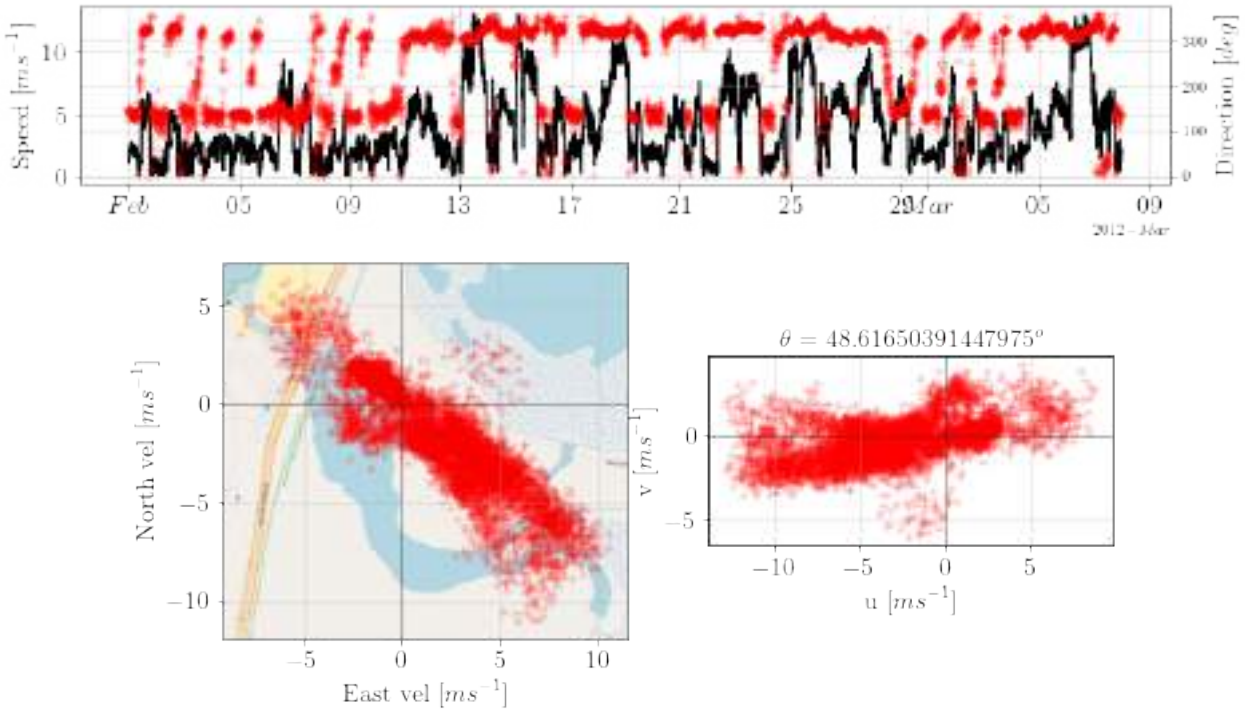

Figure 8: Time-series of wind velocity magnitude and direction. Wind velocity in North-East coordinates over the Pescadero map and in (u,v) coordinates.

4.4 Analysis techniques

4.4.1 Stratification

To represent stratification we used buoyancy frequency, defined as (Kundu et al., 2015):

$$N^2 = -(g/\rho)(\partial\rho/\partial z) \tag{1}$$

where ρ is the density of the fluid, g is 9.81 m/s^2 and z is the depth. This equation is representing the water column stability, which increases or decreases as the fluid is more or less stratified. The potential energy anomaly was calculated to observe the behavior of density in the water column. It represents the work per volume required to completely mix the water column and is calculated using the equation shown by Simpson et al. (1985):

$$\phi = \frac{1}{h}\int_0^h (\bar{\rho} - \rho) g z dz \tag{2}$$

where $\bar{\rho}$ is the average density and h is the total depth. The discretization was made according to the number of sensors that each location had and considering each layer's limits as the corresponding upper and lower sensors and the density for the whole layer as the upper one. We employed the potential energy anomaly (ϕ) as a diagnostic tool to assess the stratification of the water column before and after a wind event, thereby characterizing the state of the water column under conditions of zero wind stress and investigating the presence of mixing. Furthermore, we calculated the buoyancy frequency (N^2) during wind events to examine its relationship with density and velocity profiles.

4.4.2 Wind stress

The wind shear stress was calculated following Read et al. (2011):

$$\tau_w = \rho_{air} C_D U_{10}^2 \tag{3}$$

Where ρ_{air} is the density of air (1.2 kg/m^3) and C_D, the drag coefficient, as defined by Large and Pond (1981), was set at 0.0012 for wind velocities ranging from 4 to 11 m/s. Since the measured wind speeds in our study were below 11 m/s and the results demonstrated insensitivity to C_D, we adopted the value of 0.0012. This choice enables a direct comparison of our observations with other studies that utilized a constant C_D value, ensuring consistency across the literature. U_{10} is the adjusted wind speed at 10 meters high, and it was obtained by the log-law fit:

$$U_{10} = U_z(1 - \frac{\sqrt{C_D}}{\kappa} \ln \frac{10}{z})^{-1} \tag{4}$$

with $\kappa = 0.4$ as the Von Karmann coefficient and z = 3 m, the height of our wind measurements.

To study the response of the stratified layers to a wind impulse and identify the upwelling we used the Wedderburn number (Imberger and Hamblin, 1982):

$$W = \frac{g' h_1^2}{L u_*^2} \tag{5}$$

where L is the estuary length, h_1 is the depth of the surface layer, u_* is the friction velocity and g' is the reduced gravity. h_1 was estimated as the 30% of the DC's total depth (Fig. 9), L as 392 m, and for u_* and g' were used Eq. 6 and Eq. 7, which parameters of ρ_{bottom} and $\rho_{surface}$ are the densities in DC1 and DC4 respectively (see Table 1) and τ_w is from Eq. 3.

$$g' = \frac{\rho_{bottom} - \rho_{surface}}{\rho_{surface}} g \tag{6}$$

$$u_*^2 = \frac{\tau_w}{\rho_{surface}} \tag{7}$$

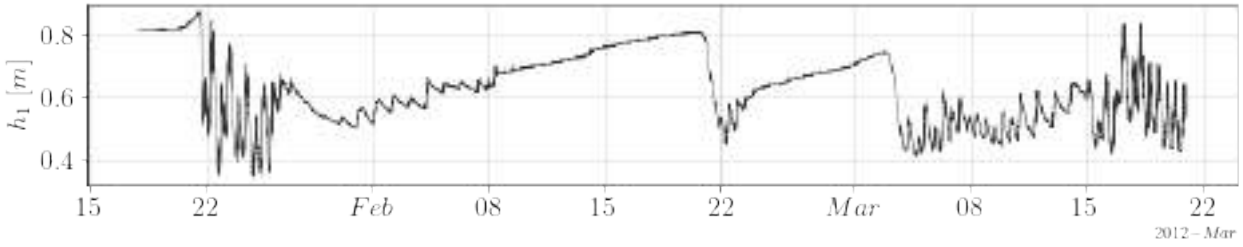

Figure 9: Time-series of 0.3 times the total depth of the estuary at the location DC.

To analyze the relationship between wind stress and density, we standardized and normalized the signals and applied cross-correlation. Cross-correlation between wind stress and density signals is used to find the time lag (phasing) between both and their level of correlation along the locations (propagation) measured in the estuary. Also, after commencement of the stress, the tilt of the interface takes $1/4$ of the internal wave period T_1 (Stevens and Imberger, 1996):

$$T_1 = \frac{2L}{\sqrt{(\frac{g' h_1 h_2}{h_1 + h_2})}} \tag{8}$$

where h_2 is the lower layer thickness, for a two layer approximation. The period T_1 is an important parameter as it characterizes the system's recovery or relaxation subsequent to a wind event.

4.4.3 Surface fluctuations analysis

To analyze what was happening on the surface, a frequency spectral analysis was carried out in order to identify the most important processes that affect the water level. First, Welch (1967) method was applied to reduce the data noise. This is a method for the estimation of power spectra using the fast Fourier transform. Then there was applied a detrend for avoiding the effects of the increase in water level. Finally, in order to detect transient events in the data and to avoid discontinuities at the beginning and the end of the analyzed data, before applying the frequency spectral analysis, the signal was multiplied by a quadratic window:

$$w[n] = \left(\frac{n - N/2}{N/2} \right)^2 ; 0 \leq n \leq N \tag{9}$$

where N is a positive integer.

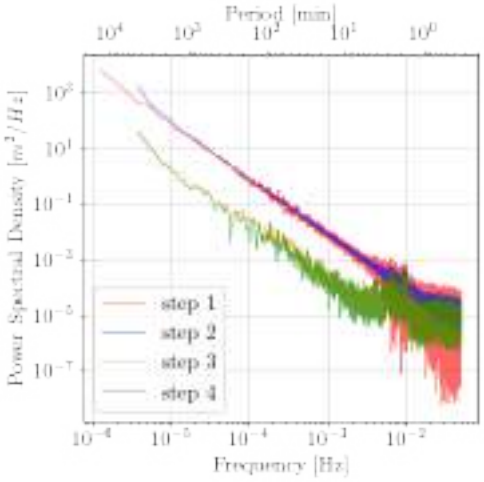

Figure 10: Step 1: Raw frequency spectral analysis. Step 2: Frequency spectral analysis using Welch (1967) method. Step 3: Frequency spectral analysis with a noise reduction and a detrend applied. Step 4: The obtained signal from step 3 is multiplied by a quadratic window shown in Eq. 9. Figure just to show the steps of the method and what is doing to the data.

To complement this information, an analysis of the wavelet transform was carried out using the Python package PyWavelets (Lee et al., 2019). The one-dimensional continuous wavelet transform was applied to the DC surface height data using the first-order Gaussian derivative family for a period range between 10 s and 2.8 min, we limited the frequencies to highlight what is important. This, in order to identify important events and other external phenomena, such as a wave overtopping the sandbar due to high tide. This analysis delivers coefficients that are a function of scale and position and that serve as a scalogram to visualize the wavelet.

To carry out a more detailed visual analysis, the standardized heights were obtained at the NM and DC points, first applying a linear detrend in a window of time and then dividing the data by the standard deviation. This

is for comparing results on the same scale. All the mentioned data were plotted according to local time, to analyze visually considering the factors that affect day and night as temperature and wind.

5 Results

The Pescadero Estuary, located at the confluence of Pescadero Creek and Butano Creek on the California coast, is a small and highly stratified estuary. It is characterized by an intermittently opening and closing inlet, where a sandbar acts as a barrier between the estuary and the sea. During the dry season, the sandbar closes the inlet, transforming the estuary into a stratified lagoon.

Field measurements were conducted between 17 Jan. 2012 and 21 Mar. 2012, capturing the estuary's conditions during this period. In Fig. 11 is shown the main data captured in the field campaign period. Fig. 11A shows the density in the watercolumn with the water level, both in DC location. Fig. 11B shows wind velocity in $u - v$ coordinates, where v is the cross-estuary direction and u is the along-estuary direction, in which offshore is positive and onshore is negative. Fig. 11C shows tidal height in MLLW datum and significant wave height. Fig. 11D shows the discharge of the Pescadero Creek. Tidal height, significant wave height and discharge are data external to the campaign.

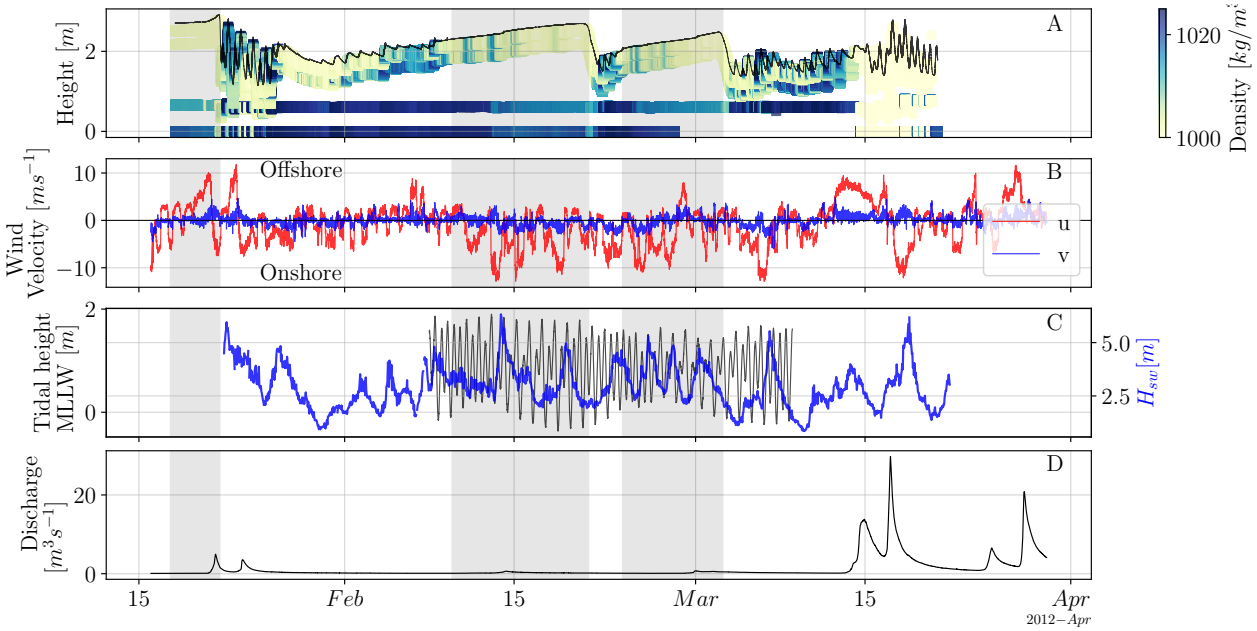

Figure 11: Time-series windowing the closed state of (A) colormap of density in DC location in the water column height, where the black line represents the water level; (B) wind speed in u and v direction; (C) tidal height in MLLW datum (black line) and significant wave height (blue line); (D) discharge.

The inlet was initially closed when the sensors were installed and remained closed until 21 Jan. 2012. Subsequently, the inlet closed again on 07 Feb. 2012 and reopened on 21 Feb. The estuary experienced its third closure on 24 Feb., which persisted until 3 Mar. (Fig. 11A).

When the mouth closes in Pescadero the flow of water between the estuary and the sea is significantly reduced, almost completely blocked, event that is presented as a decrease of density at surface and a stabilization of estuarine height (Fig. 11A). This restricted exchange isolates the estuary from the influence of oceanic

processes and creates a more confined waterbody. One consequence of the inlet closure is the establishment of stratification within the estuary. In Fig. 11A we observe lighter freshwater sitting atop denser saltwater.

Wind speed is higher during the closed state periods (Fig. 11B), not necessarily due to any important factor in our study, but it does influence how the estuary behaves in the closed state. The tidal behavior looks normal as does the significant wave height (Fig. 11C). Fig. 11D shows that discharge can change the estuary behavior (Fig. 11A), as on 21 Jan., a slight increase in discharge helped to increase the water level, and then opening the sand bar. Small increases in flow are observed on 14 Feb. and 1 Mar., which are not as significant but may affect when the swell is restricted.

5.1 Conditions observed during the closed state

Abrupt decreases in water level that were proceeded by a slow increase in the estuarine water level without tidal influence were identified as mouth openings and when tidal energy is not visible at the water level there is a mouth closure. We observed that the inlet opened three times and in each one there are abrupt density changes in the water column along with other important conditions that we are going to address below.

5.1.1 Wind in the estuary

In Fig. 12 the wind is mainly bidirectional and when it goes onshore the magnitude is bigger. Directions between 300 and 360 degrees come from the ocean and the wind that blows from 100 to 170 degrees comes from inland. This form is due to the topography of Pescadero which has an escarpment at the south of the inlet, protecting the mouth. Also, the marsh occupies a low valley, which narrows the paths of wind flow. For the along-estuary velocity, (u) we observe that the maximum velocities reach between 10 and -10 m/s approximately (Fig. 13). In the cross-estuary velocity, (v) we observed just a few spikes where the maximum velocity was reached, at approximately 5 and -5 m/s.

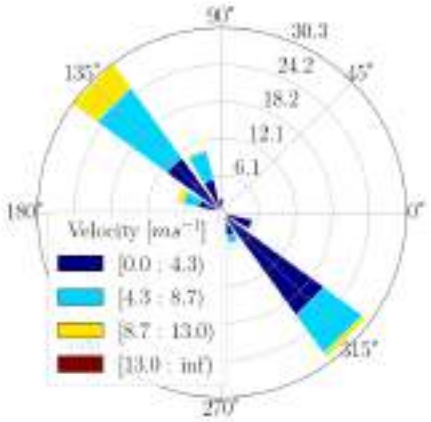

Figure 12: Windrose of the data collected in Pescadero from 15 Jan. to 20 Mar. Maximum speed registered in the studied period was 13.02 m/s

5.1.2 Evolution of density structure

Pescadero estuary is characterized by having a strong thermohaline stratification in its closed state. Fig. 14 shows the temperature (Fig. 14A), salinity (Fig. 14B), density with height above the bed (Fig. 14C) and

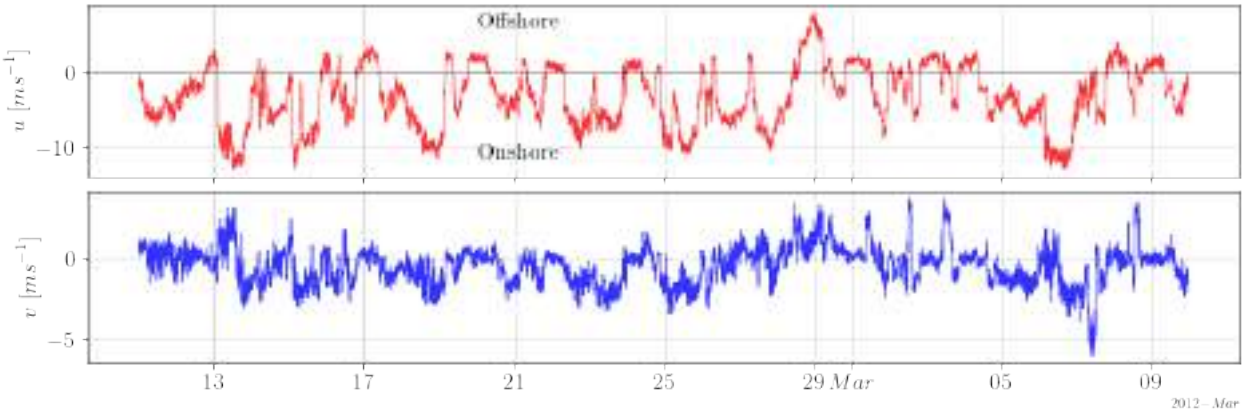

Figure 13: Time-series of wind speed in u and v direction (see Fig. 8).

the change of water level in time (Fig. 14D). When the estuary inlet starts closing, temperature and salinity acquire different values on the top and bottom of the lagoon, increasing density change in the vertical (Largier et al., 2015), Fig. 14C is showing this, when the inlet starts to close between 15 Feb. and 8 Feb. The density in the top layer (sensors 1 and 2) lowers and the density in the bottom layer (sensors 3 and 4) increases, while the water level stabilize. The difference in salinity and temperature it is also noticeable in the shadowed parts of the Fig. 14A and 14B.

We defined the closed state at the estuary when the depth's change in time $\Delta h/\Delta t$, with $\Delta t = 10$ hours, is positive and less than 0.01 m/h for more than a day (Fig. 14D), meaning that the lagoon is filling with fresh water, increasing its level, and with a low influence from the sea. In that context Pescadero is in closed state three times: in mid January, in mid February, and in late February/early March where the first one is at the start of the time series, not including the initial closure. The differences between these three closures are that the first has the highest water level, and the second and third closures never get to the same depth.

It is known that the 21 Feb. breach of the bar was artificial (Williams, 2014), openings that according to Behrens et al. (2013) would be less effective in keeping the mouth open than those that developed naturally, as in this case when the estuary is in an open state for just a couple days. The 3 Mar. barrier breach is believed to have occurred naturally.

The sand bar that forms at the inlet of the estuary contains the freshwater inflow and does not allow the waves to enter, which could explain the salinity decrease in time in the sensors 1 and 2 during closed state in the shadowed period (Fig. 14B). At the same time, during high tide the waves could be overtopping the sand bar (Laudier et al., 2011), contributing to the salinity in the system. This, depending on the magnitude of the intrusion, could affect the stratification of the entire estuary. Fig. 14D shows that in 14 Feb. and 1 Mar there was an faster increase in water level, which was already increasing showing positive values in dh/dt.

In the time series, we observed during the closed state the temperature and salinity were stratified (Fig. 14). We observed a lower and non-stable temperature at the surface (Sensors 3 and 4 in Fig. 14) due to the cold season and the following diurnal temperature changes. The temperature at the bottom (Sensors 1 and 2 in Fig. 14) is more stable, but still being influenced by daily changes and other external factors, indicating for example an abrupt fall on 13 Feb., followed by another increase. The bottom salinity is also steady most of the time and is generally decreasing. Fig. 15 shows the correlation between salinity and temperature with density.

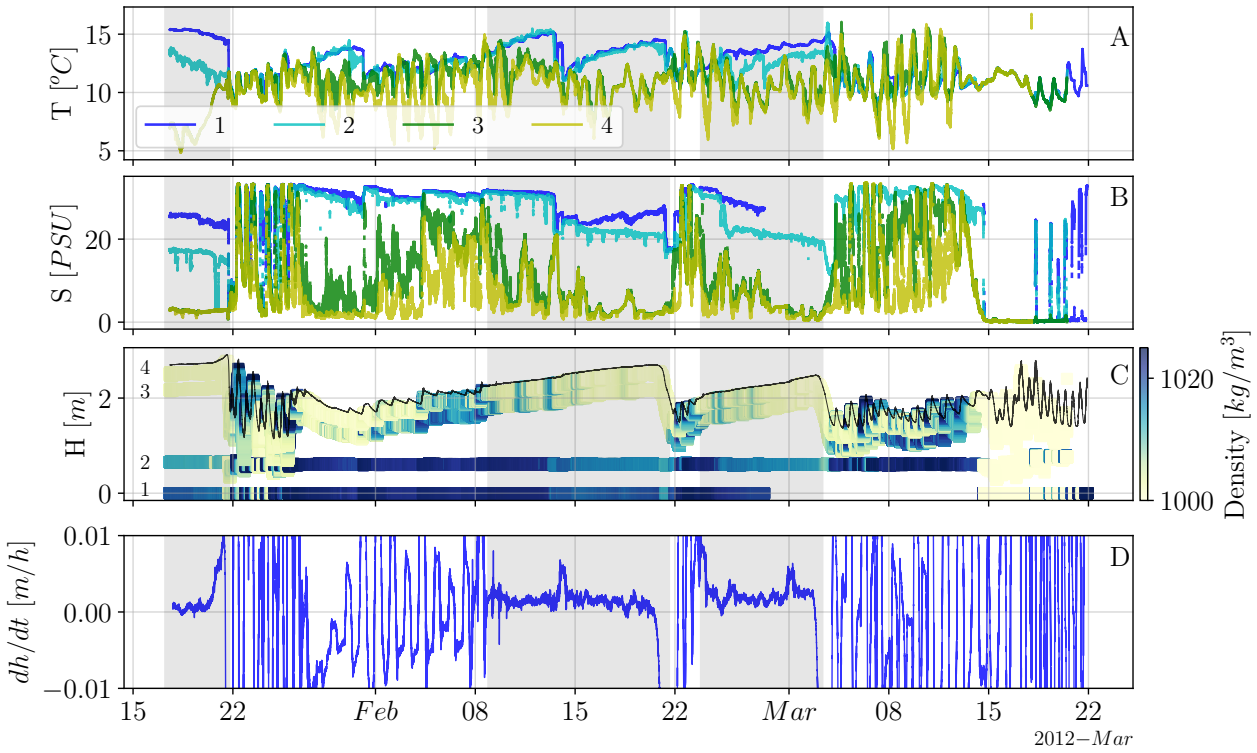

Figure 14: Time-series windowing closed state of (A) temperature and (B) salinity in NM, where 1 is the deepest sensor and 4 the shallowest; (C) colormap of density in NM with height above bed, showing the position of each sensor, where the black line represents the water level, and (D) the change of the water level in a 10-hour frame.

The correlation between salinity and density is clear, while temperature is not an important factor in density.

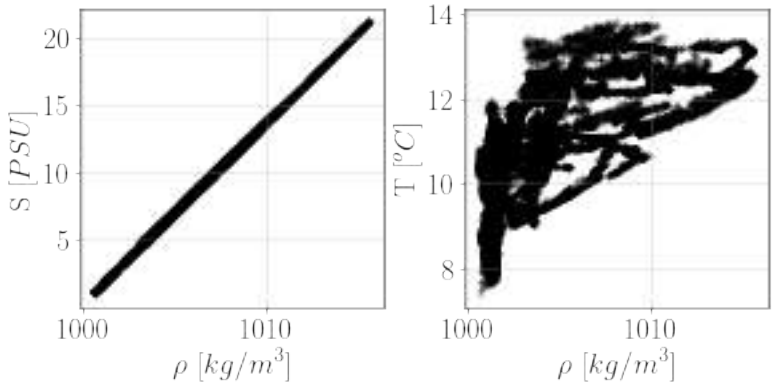

Figure 15: Salinity and temperature versus density at station DC (sensor 3) from 11 Feb. to 21 Feb.

In 16 Feb. we observed three layers in the density structure with the upper layer getting thicker upstream. In Fig. 16 there is the longitudinal view of the estuary densities from the profiles and the moorings. The moment the profiles were made (16 Feb. at 5 pm, see Fig. 13) the wind was calm, so is not causing a disturbance in

the water. Near the mouth the salinity is higher or the water column is more homogeneous. After a few days in a closed state, the estuary opened on 12 Feb. and 3 Mar. observing a decrease in water level (Fig. 14).

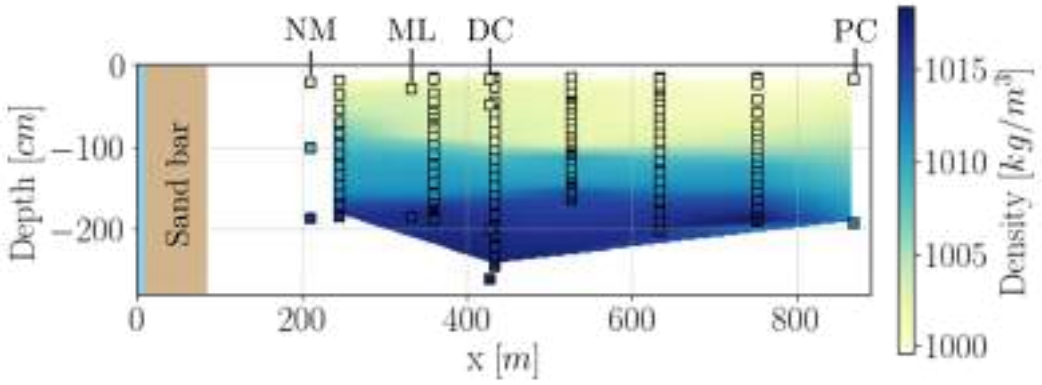

Figure 16: Along-estuary density colormap of Pescadero. Distance x is considered from the coast following the curvature of the estuary as the sensors are placed in Fig. 2.

5.1.3 Tidal and waves conditions

In Fig. 17 we have the wave conditions for Pescadero during the study period. Fig. 17A shows that when the mouth is open tidal influence is present in Pescadero, but when the mouth closes there is not an evident effect in plain sight, which does not mean there is not present. Significant wave height in the ocean goes from 2.5 m to more than 5 m approximately (Fig. 17B), though the buoy is 40 km from shore, hence, this value is employed as an indicator for coastal oceanic conditions.

The rest of the parameters (wave periods and direction) were collected from the same buoy, so they also are an approximation of the wave conditions at the coast. Dominant periods go from 5 to 20 s (Fig. 17C), while averaged periods have a range only between 7 and 10 s (Fig. 17D). The direction of the dominant period is stable at around 300 degrees most of the time, with just a peak on 29 Feb. where reaches 250 degrees (Fig. 17E).

5.1.4 Pescadero creek discharge

Pescadero estuary receives freshwater from Butano Creek and Pescadero Creek, where the latter is the one that contributes the most to the lagoon and the one we have available data. When the inlet is closed, the maximum flow recorded was $0.72\ m^3/s$, lower than the usual for winters in California, presenting two small increases in flow (Fig. 18), but which, due to their low magnitude, would not be a determining factor in the rupture, considering that between July 2011 and July 2012 the maximum flow was $29.73\ m^3/s$. Even so, there is a constant inflow of fresh water that increases the estuary water level progressively.

5.1.5 Currents speed and direction

During the closed state, the wind direction is predominantly onshore and its magnitude in that direction is bigger than in the rest of the period (See Fig. 13). Surface wind stress over the closed estuary causes the upper layer to go in the same direction as the wind, and the lower layer to move in the opposite direction (Katopodes,

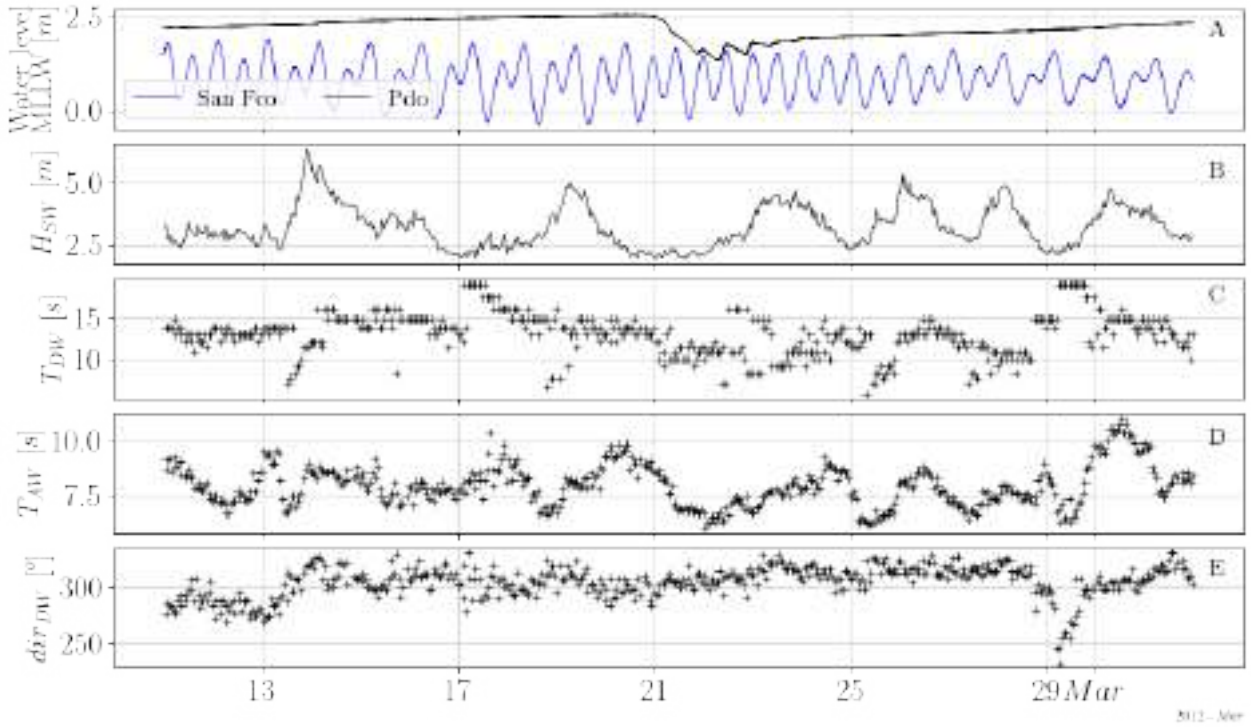

Figure 17: Time-series of (A) tidal height in San Francisco (blue) and Pescadero estuary water level (black) in MLLW datum, (B) significant wave height (H_{SW}), (C) dominant wave period (T_{DW}), (D) average wave period (T_{AW}), and (E) the direction from which the waves at the dominant period are coming (dir_{DW}).

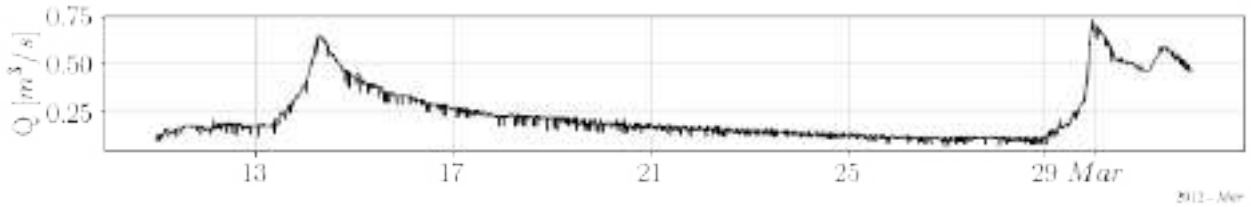

Figure 18: Time-series of freshwater flow from Pescadero Creek.

2019). Given the limitations of the ADCP sensor, measured velocities were probably never exactly at the surface, therefore, there is a range of speed observable, not showing what happens at the bottom or the surface.

5.1.6 Surface fluctuations

When the mouth is open tidal influence is present in Pescadero's water level, and when significant wave height increases the influence is also larger (Fig. 17). When the bar blocks the inlet, this causes accumulation of the upstream freshwater in the lagoon which is represented as an increase in Pescadero's water level. The closure reduces the ocean influence to be negligible to plain sight, but still could be wave overtopping the inlet sandbar. These wave overtopping events could be detected by the fluctuations in the surface present in the data, but also we have to consider the fluctuations caused by wind stress or by an increment of the discharge.

5.2 Hydrodynamic controls

The external factors expected to be affecting the estuary in a closed state are freshwater inflow, saltwater overtopping from waves, and wind stress. There are other factors involved as temperature or evaporation, but we estimated that those were negligible due to the haline stratification that dominates the estuarine structure.

5.2.1 Surface fluctuations controls

In Fig. 19 depth, wind, freshwater inflow and wave conditions for Pescadero are presented. Fig. 19A shows wind stress in the along-estuary direction during the studied period. Fig. 19B shows the wavelet frequency analysis of the DC watercolumn height. Fig. 19C shows the waterlevel in Pescadero in NM, DC and ML locations presented as standardized height (See Section 4.4.3). Fig. 19D shows the difference of the standardized depth between locations DC and ML. Fig. 19F shows the tidal height and Pescadero height in MLLW datum and significant wave height. Fig. 19G shows freshwater inflow into Pescadero.

Depth in Pescadero shows how external factors are changing the estuary. Fig. 19C shows the trend of $\hat{H}$ with a positive slope that is mostly constant. Notice that in 14 Feb. and 1 Mar. there are small changes in the velocity of waterlevel increase which coincide with the flow increase on the same date (Fig. 19G).

The wavelet frequency analysis of depth can show the effects of the waves into the lagoon, by identifying changes in its fluctuations and showing when there is the presence of certain frequencies that could represent the ocean influence. If we crossed this information with tidal behavior and significant wave height we obtain a more certain way to identify wave overtopping events. In Fig. 19 the wavelet analysis is shown between frequencies 0.2 and 0.007 Hz because this is where the wave information can be extracted more easily, since at lower frequencies no noticeable changes in the frequency density were identified.

When the estuary is open the ocean effects are very marked in the wavelet analysis (Fig. 19B). During a closed state, the effects are also evident but more slightly, with more concentrations of frequencies between 0.02 and 0.1 Hz, and we could point out that those are wave overtopping events, considering that they occur during high tide and waves (Fig. 19F). Also, they occur exclusively at high tide, and any wave height, but the events are bigger when the waves are larger. On the other hand, wave overtopping does not have a clear pattern of behavior in dh/dt (Fig. 19D) or $(\hat{H}_{DC} - \hat{H}_{ML})/\Delta x$ (Fig. 19E) when the inlet is closed.

As we notice earlier, the discharge has two increase events during the studied period (Fig. 19G). Those increases are affecting directly the surface, showing important peaks of dh/dt during those events (Fig. 19D). Also, the change of the standardized height in the horizontal ($\Delta\hat{H}/\Delta x$, Fig. 19E) showed at the beginning of the period negative values which changed to positive values after the increase of discharge, which also happens after a strong wind event and during a wave overtopping.

5.2.2 Stratification controls

In Fig. 20 density, wind, freshwater inflow and wave conditions for Pescadero are presented. Fig. 20A shows wind stress in the along-estuary direction during the studied period. Figs. 20B, 20C, 20D show density in each sensor (See Fig. 2). Fig. 20E shows the tidal height and Pescadero height in MLLW datum and significant wave height. Fig. 20F shows freshwater inflow into Pescadero.

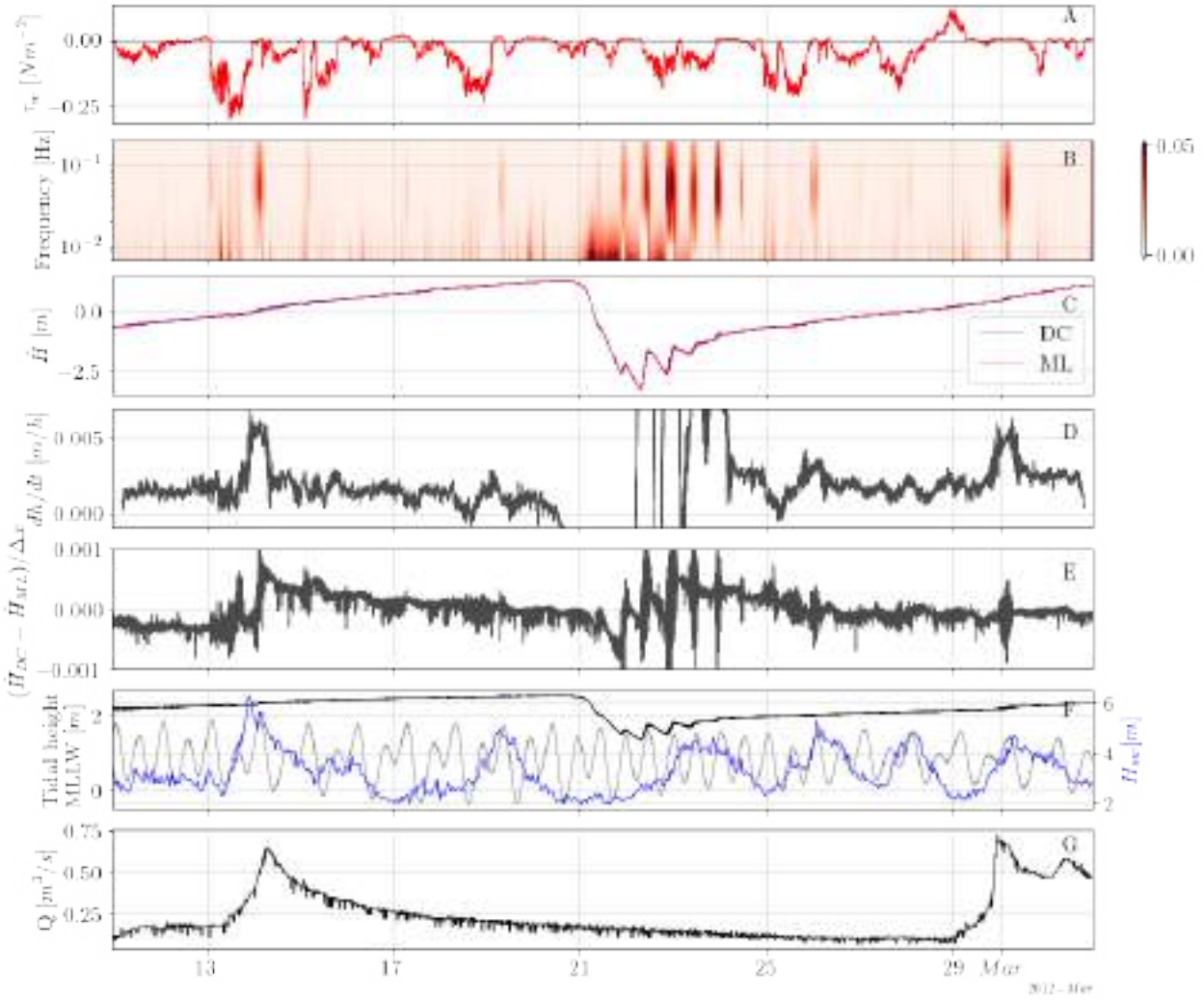

Figure 19: Time-series of (A) wind stress (τ_w), (B) depth wavelet frequency analysis at DC, (C) standardized depth ($\hat{H}$) in DC, NM, and ML locations, (D) the change of the water level in a 10-hour window (dh/dt), (E) standardized depth difference between locations DC and ML ($(\hat{H}_{DC} - \hat{H}_{ML})/\Delta x$), (F) significant wave height in Halfmoon Bay (blue), Pescadero estuary water level (black) and tidal height in San Francisco (gray) in MLLW datum, and (G) freshwater inflow of Pescadero creek (Q).

At the beginning of both periods of inlet closure (12 Feb. and 25 Feb.), there were changes in densities on the surface and in the deep layer, although the latter in smaller magnitude and fewer times (Figs. 20B, 20C and 20D). Three important wind events occurred in each period, total of six, that matches with the increase in surface densities (13, 15, 18, 25, 26 and 27 Feb.), observing that when the stress on the surface increases, so does the density in the upper layer in the three sites (NM, ML and DC). When wind forcing decreases, density tends to return to its initial state, except for the largest events at the beginning of each period, where density at the bottom is smaller after the event than before (13 Feb. event and 25 Feb. event).

Upstream freshwater inflow had two small increases in the studied period in 14 Feb. and 29 Feb. (Fig. 20F). During those events there was not an instant change in density, but we could notice a decreasing trend in

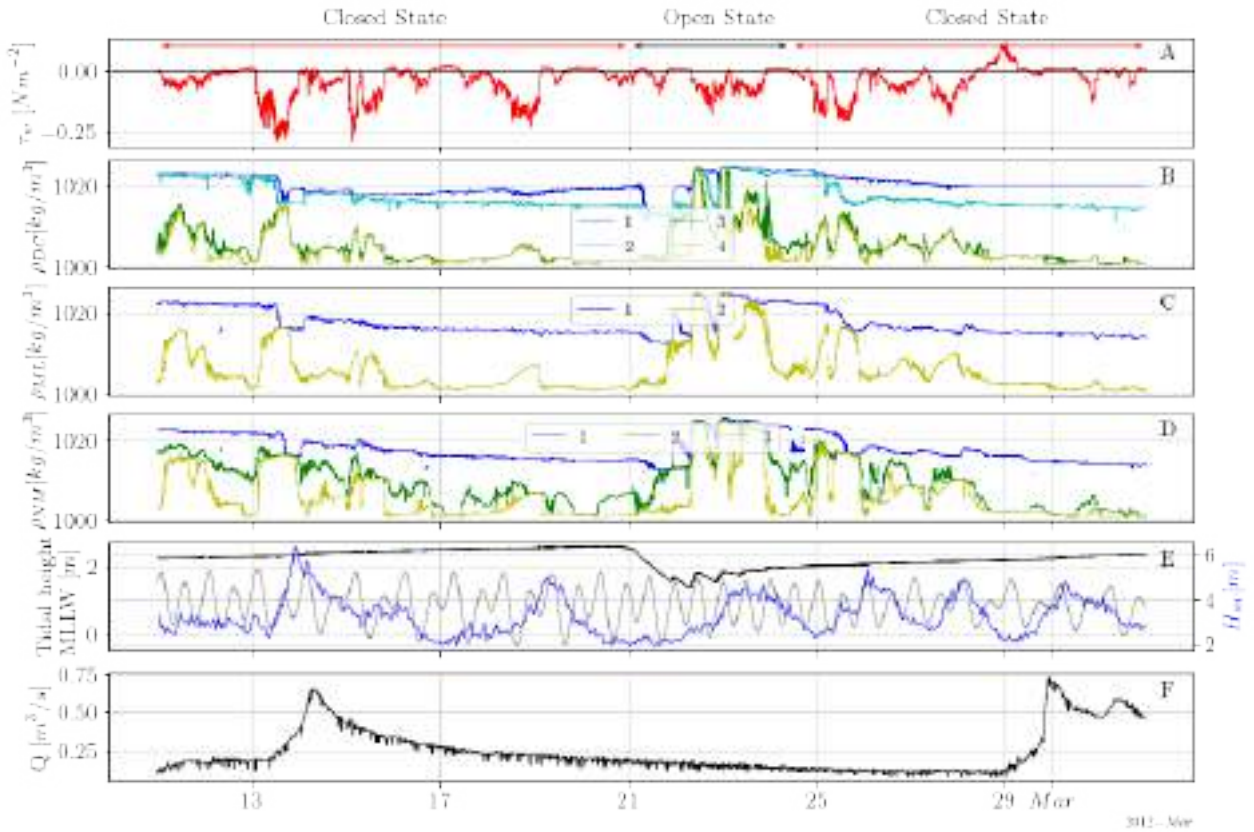

Figure 20: Time-series of (A) wind stress (τ_w), (B) DC (ρ_{DC}), (C) ML (ρ_{ML}), and (D) NM (ρ_{NM}) densities in different depths, where sensor 1 is the deepest and sensor 4 is the shallowest (The positions in the water column of the sensors are shown in Fig. 16),(E) significant wave height in Halfmoon Bay in blue (H_{sw}), Pescadero estuary water level (black) and tidal height in San Francisco (gray) in MLLW datum, and (F) freshwater inflow of Pescadero creek (Q).

density during both closed state periods. In the first period, at the DC location, unlike the others, there was an increasing trend of density, between 19 and 21 Feb., which would not be unusual considering the lower layer of DC is much deeper than the ones of NM and ML (Fig. 16), furthermore, the layer in DC with the same depth to those is the DC2 sensor (in cyan, Fig. 20A). Another change in density that is noticeable occurs in NM2 sensor (in green, Fig. 20D) between 13 Feb. and 17 Feb., just before and after there was an increase in discharge. Density went from around 1015 kg/m^3 to almost 1000 kg/m^3, notice there was also a wind event during that period, but we can separate the effects considering wind increase density.

Another external factor potentially influencing stratification involves the ingress of seawater into the estuary through wave overtopping of the inlet sandbar. While significant wave height and tidal height might indicate instances of wave overtopping during periods of elevated tides and wave activity, the absence of high waves doesn't preclude wave overtopping during high tide occurrences alone. In order to identify wave overtopping in the estuary there must be fluctuations in the surface and is expected an increase in density. Even though we do not observe important increases in density that indicate an important saltwater input, except for the trend in DC lower layer mentioned earlier (Fig. 20B), so we cannot know when happens. Anyways, there are small

changes in density both on the bottom and on the surface.

What is observed in Fig. 20B, 20C and 20D in general is, first, density fluctuations at the surface (yellow line) but without causing important changes on 14 Feb., 16 Feb., 19 Feb., 20 Feb., 26 Feb., 27 Feb., and 1 Mar, while there was high tide and sometimes high waves, but all of them happened right after a wind event or during an increase of discharge (Fig. 20A and 20D), so we can't assume that one factor or another is causing it. Second, in the bottom (blue line in Fig. 20B, 20C and 20D), we observed some density increases that were momentary on 15 Feb., 26 Feb., 27 Feb. and 28 Feb. during high tide, and mainly noticeable in NM, which is the closest location to the inlet (Fig. 2). Those increases do not look like the increases in salinity caused by wind effects, because the salinity is bigger than before the wind event in some cases, although, as this still happens when there was a wind event we cannot attribute it just to wave overtopping. Third, there was a continuous increase in DC1 (bottom layer) that happened after an important decrease in salinity due to a wind event, between 19 and 21 Feb..

5.3 Wind-driven effects

Changes in density occur at the same time as wind events as shown in the previous section. To quantify those changes we calculated the potential energy anomaly of the water column in location NM using surface and bed CTDs and compared it to wind stress (Fig. 21). When wind stress magnitude increases (Fig. 21, τ_w), potential energy anomaly decreases (Fig. 21, ϕ), except when there are positive values like on 28 Feb. and 29 Feb, when there was no change in potential energy anomaly. However, the potential energy anomaly does not have the same behavior in wind events of the same magnitude, and, in time, wind decreases its effect on the potential energy anomaly, only reaching 0 at the first wind event of each period (14 and 25 Feb.). In addition, after those events there is a decrease in potential energy anomaly when wind stress is zero (See black dots in Fig. 21), probably showing a change in their stratification structure after those events.

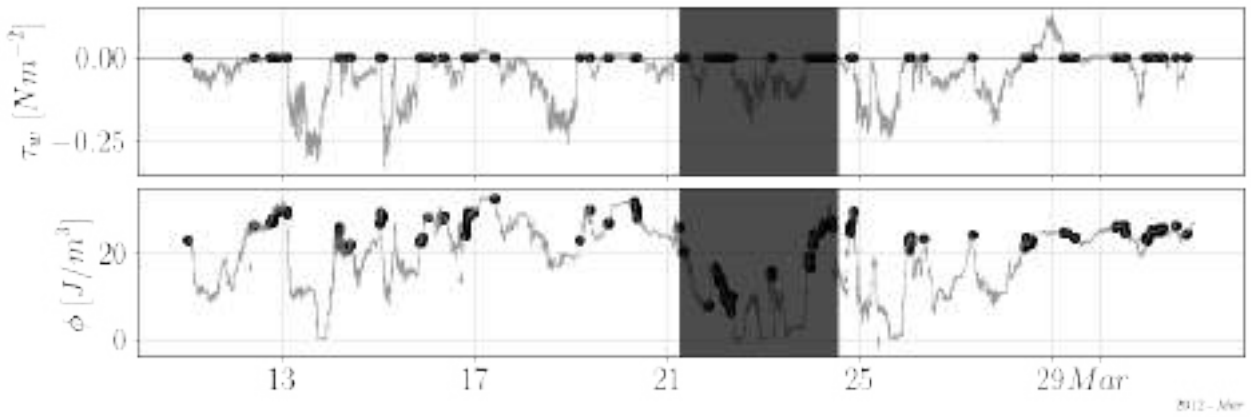

Figure 21: Time-series of wind stress (τ_w), and potential energy anomaly (ϕ). Dots are instants when wind stress is zero. The shaded window is when the estuary is in an open state.

For further understanding, we calculated the Wedderburn number to observe if there was upwelling due to wind events. As we did not have the thickness of the epilimnion we estimated a range of positions for the pycnocline. This range started right after the first CTD, the deeper one (in black), and ended in the second CTD (in grey) (Fig. 22). Also, we marked with a star where was the epilimnion limit on 16 Feb., when we

had more information on the density (Fig. 16), which could be changing in time. As we are working with a range of values, we considered a partial upwelling when just the upper boundary reaches W=1 and full upwelling when both boundaries reach that value. In each period we noticed one full upwelling event and two partial upwelling events, for a total of six upwelling events observed in the studied period, always the first one being fully upwelled (Fig. 22). After full upwelling events, density at the bottom of the water column did not come back to its original values from before the event.

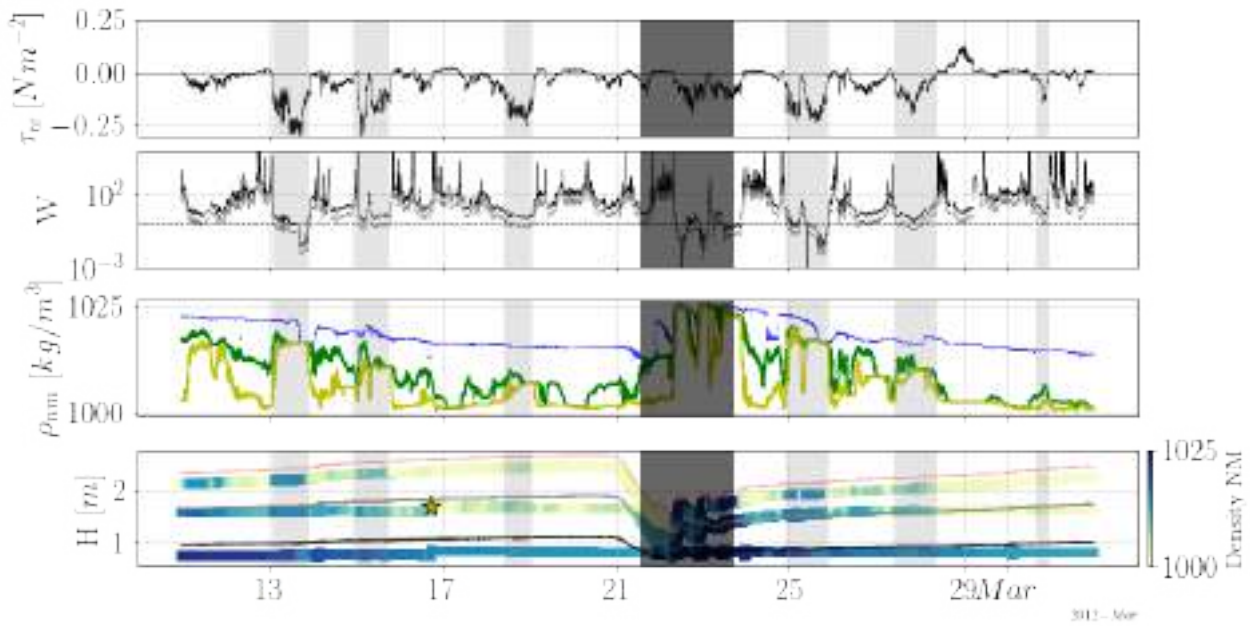

Figure 22: Time-series of wind surface shear stress (τ_w), Wedderburn number (W) where the dashed line shows W=1 and black and gray lines show W obtained at the lower and upper part of the selected window respectively, density at the bottom (blue), middle (green), and top (yellow) of the water column in NM location (ρ_{nm}) (see Fig. 16 for sensors positions), and colormap of density in time-space at each sensor of location NM with the black and gray line that limit the lower and upper part of the window of possible values for top layer width. The dark shadowed window is when the estuary is in the open state. Light-shadowed windows are when the upwelling events were observed. Redline is the water level, and the star indicates where the surface layer ends according to Fig. 16.

In Fig. 23 we observe how density at the surface is getting more resilient to wind effects over time. The three wind events in the first period are similar in magnitude, but the increase in density that they trigger is each time smaller. What's more, we notice a small wind stress event at the beginning of the time series (11 Feb.) that increased density three times more than the last wind event in the period (18-19 Feb.). Density changes in the vertical ($\Delta\rho/\Delta z$) reached 0 at the first wind event of each period, but then, after the event, $\Delta\rho/\Delta z$ went steadier and did not reach 0 again during the period.

The first important wind event started on 13 Feb. at 2 a.m. and the first location that was affected was NM, then ML, and finally DC. The latter is shown with the change of density along the estuary (Fig. 23) where there are negative values of $\Delta\rho/\Delta x$ almost all the time, meaning higher values of ρ_{NM} than of ρ_{DC}. When the wind starts to blow there is an increase in $\Delta\rho/\Delta x$ magnitude, and after reaching the peak the value decreases again to zero and stays there if the wind speed is constant. If wind speed decreases there is

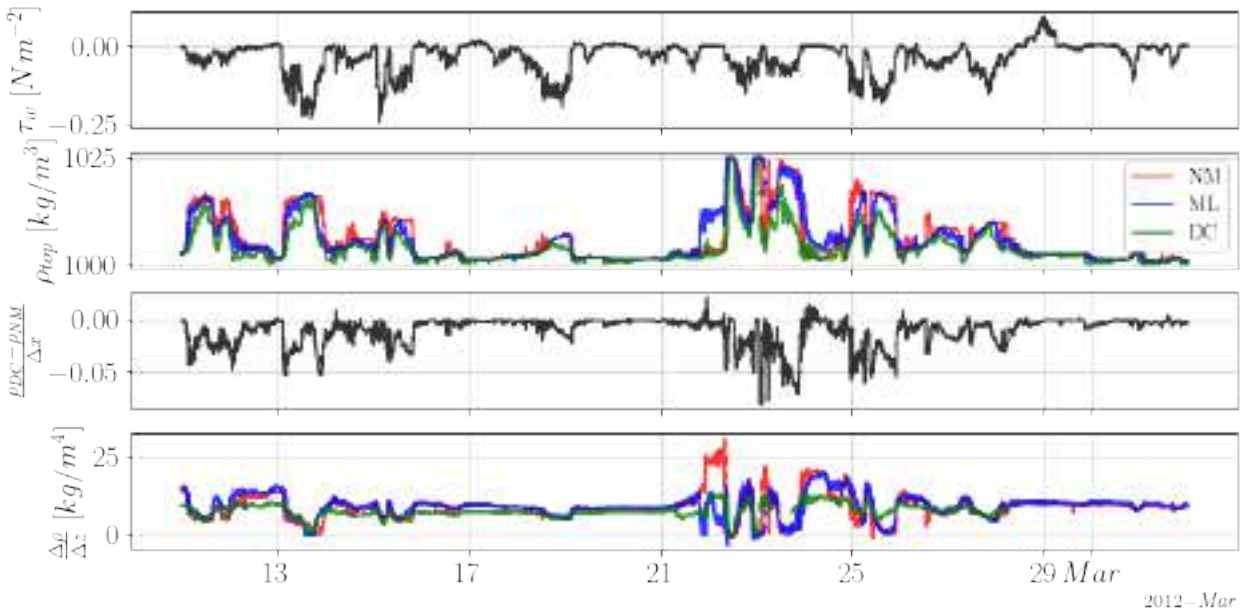

Figure 23: Time-series of wind shear stress at the surface (τ_w), surface densities in locations NM, ML, and DC (ρ_{top}), density change between locations DC and NM at the surface ($\frac{\rho_{DC}-\rho_{NM}}{\Delta x}$), and density change between surface and bottom in locations NM, ML, and DC ($\frac{\Delta\rho}{\Delta z}$ $[kg/m^4]$).

another increase in $\Delta\rho/\Delta x$ magnitude, showing that the wind stops influencing DC location first and then NM.

To quantify the time difference between the moment the wind started blowing and the density started changing at the different CTD locations, we calculated by visual inspection how long it took for the wind to affect density at different points. To achieve this, we considered the moment that density just started to change into a trend after the wind started or stopped blowing. Also, to compare the obtained values we calculated the cross-correlation, between density and wind stress, after normalizing and standardizing both signals. We obtained the values of the first wind event, and how long took to start and finish, and for the cross-correlation, we added the total of the first-period lag.

Table 2 shows that surface sensors (NM3, DC4, and ML2) had no delay with the cross-correlation method and did have it in the visual inspection. NM3 was the last sensor that started to change after the wind stress started, but it increased faster than the others, a fact that is observed in Fig. 23 for ρ_{top}. Also, we observed that the sensor that took longer to return to its initial value was NM3, then ML2 and DC4.

If we compared Table 2 values to the response tilt time, obtained as the fourth part of the internal wave period, that is 11.75 ± 2.72 min, we observe that it is the most approximate to the values of the total period obtained by cross-correlation at the surface, but they are the double of it. Also, at the beginning of the event by visual inspection DC4 takes 10 minutes to start changing which, considering that DC is at the center of the estuary, could be a representative value of the response tilt time in Pescadero.

Surface wind stress over the closed estuary results in the upper layer moving in alignment with the wind, while the lower layer moves in the opposite direction (Katopodes, 2019). Given the limitations of the ADCP sensor, velocities near the surface were not always captured, therefore, we observed a range of speed, not

Table 2: Lag obtained by cross-correlation method and visual inspection. "Start" columns mean that lag was calculated only when the wind stress magnitude was increasing at the first event, and "end" columns mean that lag was obtained when the wind stress magnitude was decreasing at the first event.

Method	Cross-correlation				Visual inspection		
Sensor	Start	End	Total event	Total period	Start	End	Total event
NM1	252 min	132 min	354 min	384 min	810 min	420 min	615 min
NM3	0 min	0 min	0 min	36 min	30 min	225 min	127 min
DC1	36 min	0 min	258 min	732 min	630 min	30 min	330 min
DC4	0 min	0 min	0 min	30 min	10 min	0 min	5 min
ML1	54 min	174 min	450 min	600 min	615 min	500 min	557 min
ML2	0 min	0 min	0 min	24 min	0 min	55 min	27 min

showing what happens at the bottom or the surface. Fig. 24 shows that the along-estuary speeds (u) increase in proportion to the wind stress, but in opposite direction. The wind is also influencing cross-estuary velocity (v), but with less intensity due to the wind's main velocities. Vertical velocity (w) presents fluctuations and some negative or positive peaks during wind events or after in some cases.

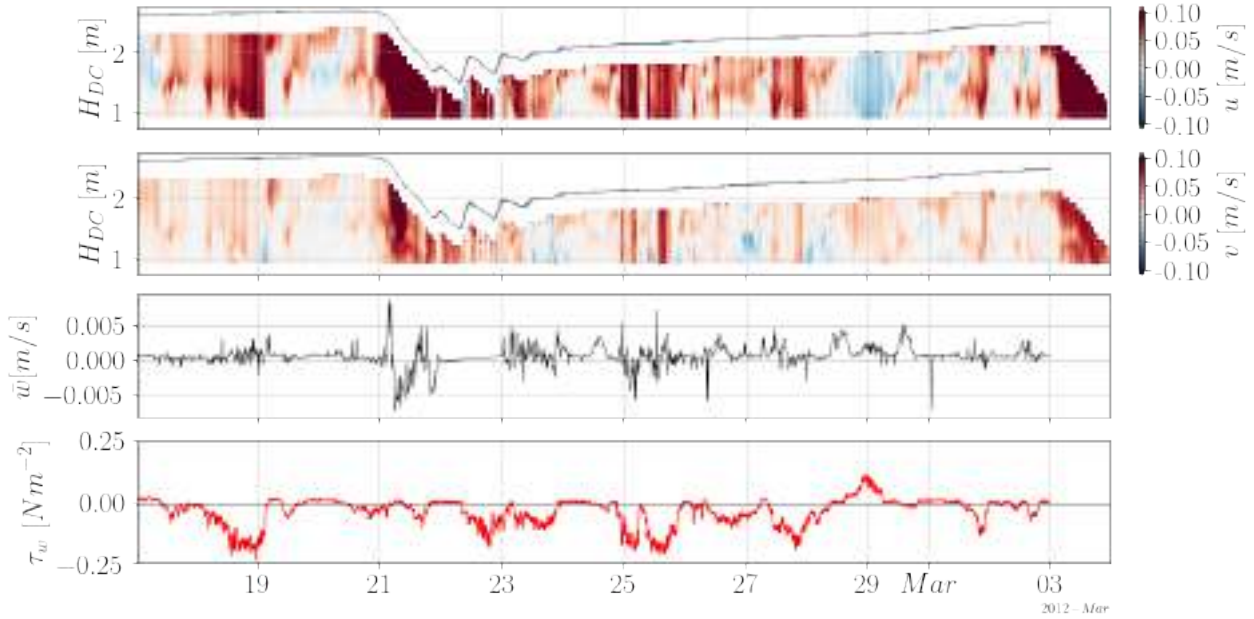

Figure 24: Time-series of: u and v in the vertical, averaged vertical velocity, and wind stress.

The observed dynamic of the upper velocity at the window shown in Fig. 24 is such that when wind stress has positive velocity, considering positive the direction of the streamflow, the along-estuary water velocity is negative and vice versa. The magnitude of wind stress does not change this behavior along time, but as the water level increase, the estuarine velocity gets smaller for the same wind-stress magnitude. However, when wind stress is very small the dynamic change, and the upper along-estuary velocity at the window goes in the same direction as the wind stress at the surface like in 20 Feb. and 1 Mar..

For the average vertical velocity in the water column ($\hat{w}$) (Fig. 24) we observe mainly positive values (upwards), but there is no interesting behavior in it until the second period when we observed more changes, other than small fluctuations during a wind event. We could observe important peaks when the wind was starting to blow and, in some cases, right after the wind finished, showing that layers are going upwards at that moment (26 Feb. and 27 Feb.). Also, we observed negative values during the first wind event on the second period, showing probably that the surface tilt is returning to its initial state.

To observe in detail the behavior of the water column, densities and velocity profiles for each sensor were plotted in certain instants in the first wind event of the second period, between 24 and 26 Feb. (Fig. 25). This wind event is characterized by two wind increases and a period in the middle with small wind stress that lasted 3 hours approximately. The profiles before the event, during the first increase, the middle period, the second increase, and after the event were plotted.

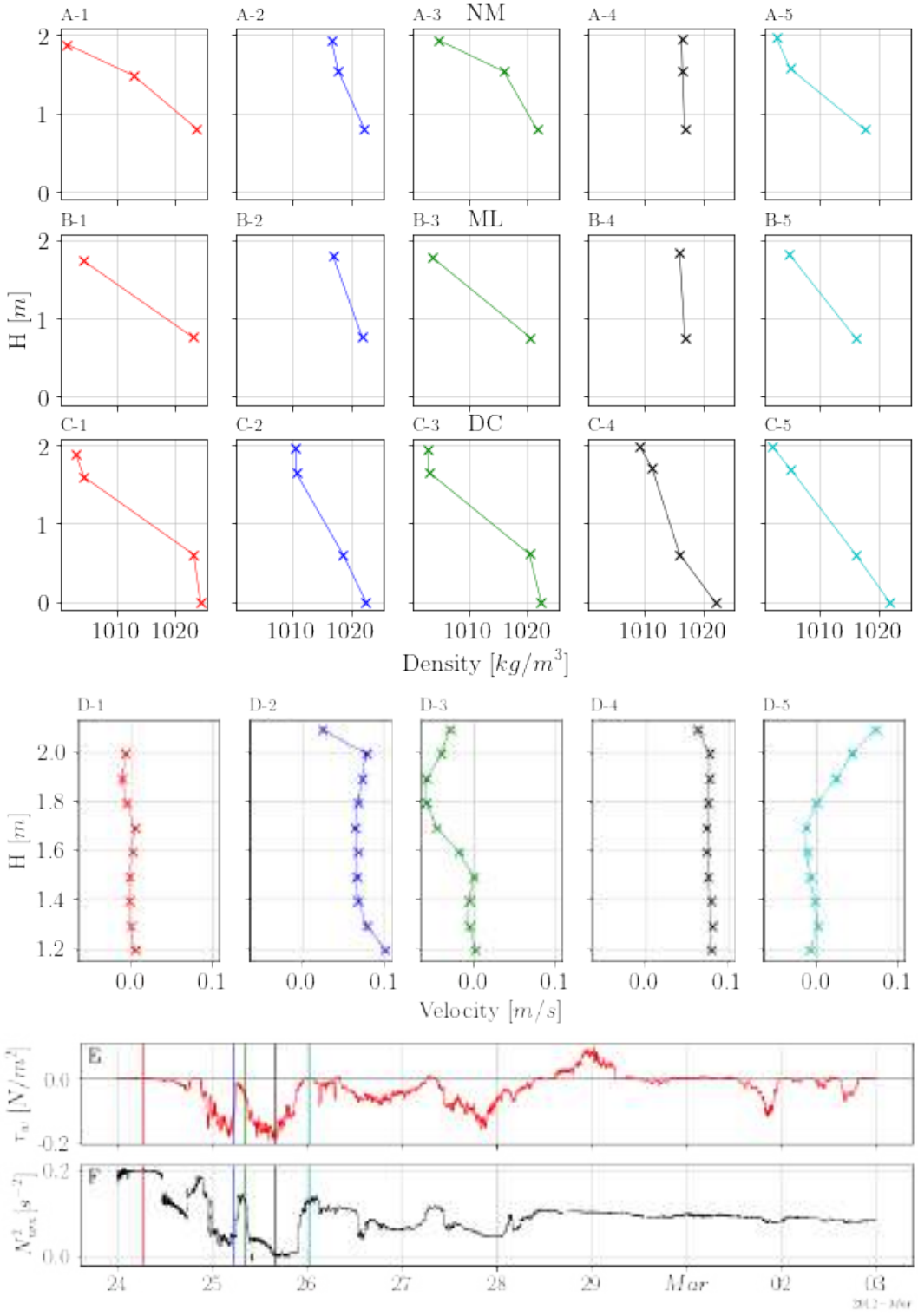

Figure 25: Density profiles at locations (A) NM, (B) ML and (C) DC, and (D) along-estuary water velocity profiles of 5 moments before, during, and after a full upwelling event, and time-series of (E) wind stress and (F) buoyancy frequency showing the plotted instants.

Before the wind event the water column is stratified and the along-estuary water velocity is zero. During the first part of the event, the principal effect is the density increases near the surface and the positive velocity in all the visible part of the water column. When the wind stopped the estuary went stratified with similar values of density to the first profiles, but the u velocity had a different behavior, and went negative in the upper layer, probably showing that the water is returning to its original state or that when wind stress is too small the surface water that goes into the same direction of the wind gets thicker and starts to be detected by the ADCP. When the wind reaches its maximum the water column is less stratified than in the first increase and velocity has bigger values. The last profile (Fig. 25 D-5) shows positive velocities at the surface and as there is no wind at that moment the density profile shows a stratified estuary but less than before the event, meaning there was mixing in the water column during the wind event (Fig. 25 C-1 and C-5).

When the wind is blowing inland, shear stress causes a set up at the end of the estuary by driving water away from the free surface, increasing upstream hydrostatic pressure and causing estuarine recirculation. This causes the pycnocline to move towards the surface and increase in density where the surface layer used to be. This is what is happening in Fig. 25, where NM has been affected first and more abruptly than ML and DC, the latter being the one that changes its density the least. This may be because NM is the closest sensor to the mouth of the estuary, and therefore it is the one that detects the pycnocline first, followed by ML and DC.

Buoyancy frequency values when wind stress is zero decreased, going from 0.2 to 0.1 kg/m^3 showing less stratification after the big wind event. N^2 is steadier after the wind event and decreases less for winds of the same magnitude (Fig. 25).

In Fig. 26 there is a closer look of the behavior of the water level. First, in the wavelet analysis we observed three events of wave overtopping, which show a concentration of frequencies in the range from $2 * 10^{-2}$ to $2 * 10^{-1}$ Hz. Also, during the wind event the frequencies showed less concentration than in the wave overtopping event and in the range of frequencies between 10^{-2} and $2 * 10^{-1}$ Hz. Second, the standardized height ($\hat{H}$) showed an increase with a positive peak when the wind started blowing, which when it went stronger decreased to negative values with lots of surface fluctuations. When the wind stopped the height return to positive values near 0. This is indicating an inclination of the surface or a set up.

The change of the depth in time showed mainly positive values almost all the period (Fig. 26), meaning that the water level is increasing most of the time. The only moment when the change was negative for more than an hour occur at the beginning of the wind event. Also, at the end of the time series there is a peak of negative values with unknown cause. The difference between the standardized height of DC and ML along-estuary indicates that when this value increases, the height in ML is smaller and the height in DC is larger, and vice versa. This could be caused by both the wind and other external factors such as inflow from upstream, flow that may be entering or escaping through the sand bar, among others. In Fig. 26 at the beginning of the time series the values of $\Delta\hat{H}/\Delta x$ are oscillating slightly around 0 with a wavelength of 24 h approximately. When the wind started blowing, the values turned negative, showing that DC decreased more than ML. After the wind event, the values continued the oscillations, but with more amplitude than before.

The spectral analysis of the depth in DC, ML and NM (Fig. 27) shows that between frequencies of $4 * 10^{-3}$ and $1 * 10^{-2}$ Hz, around a period of 2 min, there is an increase in Power Spectral Density (PSD), showing us the presence of infragravity waves in Pescadero. If we add to the spectral analysis the wind stress and compare it we observed some similarities in the frequencies. Between $8 * 10^{-5}$ and $1 * 10^{-4}$ Hz there is an increase in PSD for wind and depth at NM, that is for the period around 200 min, and also between $1 * 10^{-4}$ and $1.1 * 10^{-4}$ Hz we notice peaks in wind and depth in ML and DC, that correspond to 140 min approximately.

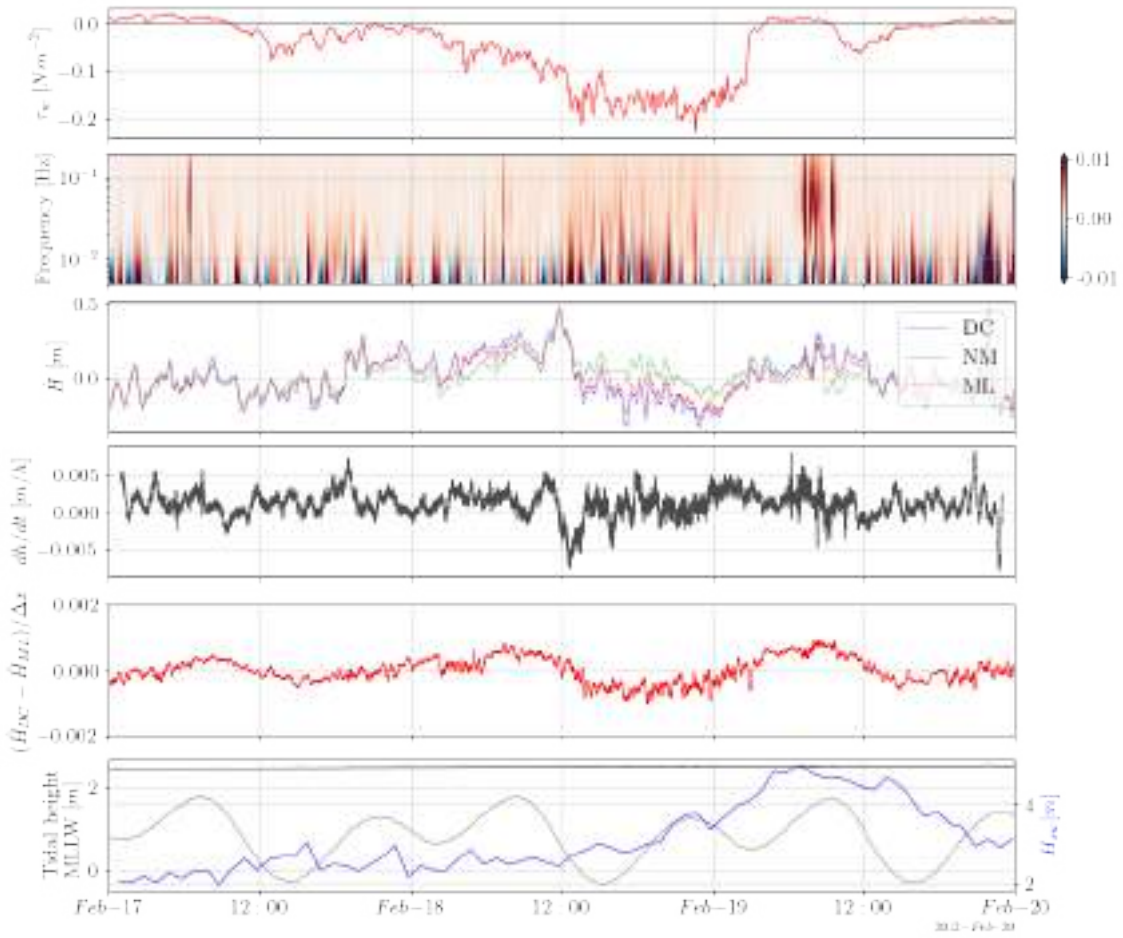

Figure 26: Time-series of wind stress (τ_w), depth wavelet frequency analysis at DC, standardized depth ($\hat{H}$) in DC and ML locations, the change of the water level in a 2-hour frame (dh/dt), standardized depth change between locations DC and ML ($(\hat{H}_{DC} - \hat{H}_{ML})/\Delta x$) with its rolling mean, and significant wave height in Halfmoon Bay (blue), Pescadero estuary water level (black) and tidal height in San Francisco (gray) in MLLW datum.

In addition we observed two peaks in wind stress between $2 * 10^{-5}$ and $5 * 10^{-5}$ Hz, that is between 700 and 300 min, while in the depth spectrum we observed some increases in the three sites for the same range but with less significance.

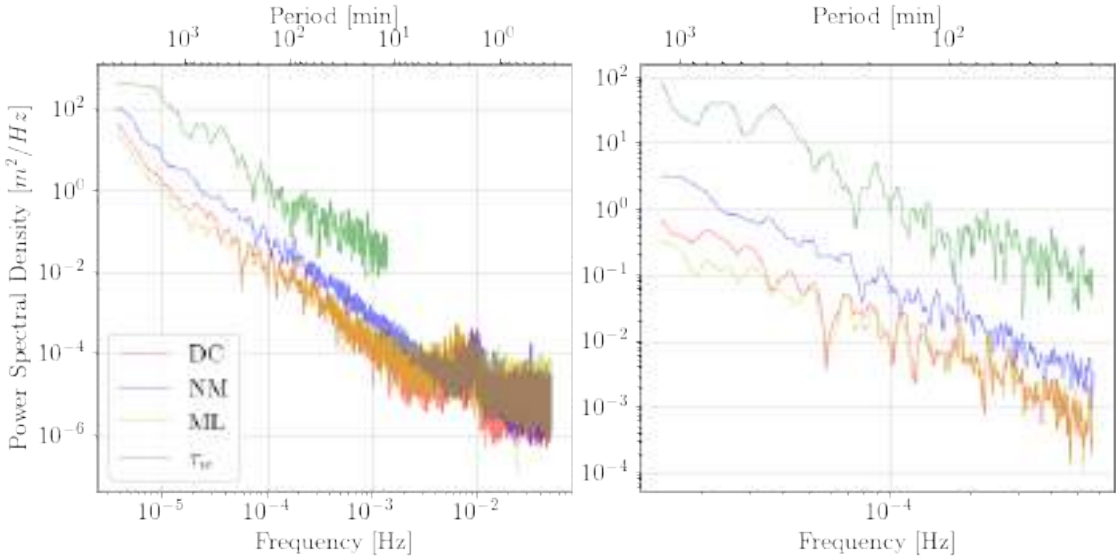

Figure 27: Frequency spectra of water level fluctuations in the estuary at sites in NM, DC and ML, and of wind surface stress between 11 Feb. and 20 Feb. with a close up of the lower frequencies.

6 Discussion

When the mouth of an estuary is closed, it can become vertically stratified due to the freshwater input and the occasional wave overtopping of saline water. In such circumstances, it becomes difficult to energize the water column. However, external factors such as wind stress on the surface, discharge and wave overtopping can cause vertical transport in the water column (Roberts et al., 2021). In the case of Pescadero, upwelling, that cause the lower layer to emerge in surface, caused vertical exchange and/or mixing due to wind-induced baroclinic conditions. As the estuary would always be saltier than the input water from the creeks, resulting in a consistently stratified water column. Nevertheless, there exists a light density/salinity gradient in Pescadero due to the freshwater input from upstream and saltwater overtopping the bar at the other end.

6.1 Estuarine structure and morphology

During the winter of 2012 Pescadero estuary received less freshwater inflow compared to other months throughout the year, leading the inlet to disconnect from the ocean. Pescadero during its closed state function as a stratified coastal lagoon with river runoff forming a surface layer of freshwater and occasionally having tidal inflows of saline water. The orientation of the bay and the shallowness result in the exposure of all the water columns to the wind stress events. In this regard, Pescadero shares many physical traits with other bar-built estuaries where the local wind forcing is the dominant driver.

Apart from the stratification, there is an along-estuary density gradient between the outlet of the creek and the mouth, due to the constant discharge of freshwater. Near the mouth, the upper layer is thinner than in the creek's outlet, because the salinity is higher in the mouth probably due to the waves that are overtopping the sandbar along with upstream continuous freshwater input.

The present study analysis reported that the major driver of mixing is wind stress and the major driver of water level variability is freshwater inflow, even in periods when is very low. In the next sections, we are going to discuss the role of other factors that affect Pescadero and its importance in stratification and water level.

6.2 Analysis methods

Wind and estuarine velocities were axis-rotated in the direction of maximum variance of water currents (See Fig. 7, Section 4.3.2), but there was also the option of doing it in the direction of wind velocity. This puts the main focus on the estuary currents instead of the wind velocity, but in this particular case, both, wind and water velocities, have a similar principal direction, so it wouldn't be a big difference between each option.

We adjusted the first cell of the ADCP data by visual inspection, using the blank space given by the ADCP, which was 0.71 m, and overlapping it with the CTD data on the same location DC. This comparison gave us the value of 0.91 m for the first cell location, which is merely an estimation of bathymetry, so it could have been a different value, bigger or smaller depending on how we had placed the overlapping. This does not affect velocity values, but we have to consider it for the positions of the layers or the profiles, but it does not make an important change in the analysis.

The closed state definition was set in a range of depth's change in time values with a 10-hour frame. The frame was selected by trial and error based on the timescale we were working on and it could change depending on the period in which the data was collected and the data collection frequency. Also, we have to consider that the opening and closures do not happen in an instant, but in a process that could last from minutes to hours, so it could be considered any instant during that process. In this case, the registered openings lasted 4, 21 and 28 hours each.

In this study, we did not consider temperature and evaporation factors. We considered that the effect of temperature was not important due to the haline stratification that dominated the estuary, but it could be studied in greater depth in future analyzes in Pescadero. Also, we didn't consider evaporation as a factor for depth changes because we are studying an estuary with a small area, and as it was winter time the air temperature was not too high to cause major impacts.

To calculate wind stress we used a drag coefficient defined by Large and Pond (1981), but according to Paugam et al. (2021) the drag coefficient C_D can be difficult to estimate in shallow water, so we have to consider the obtained C_D as an approximation in the wind stress and everything calculated with that coefficient. In future studies, there could be used other drag coefficients to observe if there is a big difference in the wind stress and other indices obtained with C_D.

The Wedderburn number was obtained with the equation for a rectangular basin defined by Monismith (1985), so it is showing us an approximated value. Despite this, it is still a good indicator to estimate the behavior of the stratification to wind stress. We could try in future research more adapted Wedderburn numbers to the Pescadero basin and compare the results with those obtained in this study.

The frequency spectral analysis only shows a general view of the most important frequencies in the dataset but does not show the specific time when this happens. This makes it a special tool to detect frequency peaks and contrasting different datasets.

6.3 Wind stress mixing

Strong wind events were an important part of estuarine dynamics in Pescadero, inducing changes in circulation and stratification. Between November and January, sporadic strong wind events were recorded, with 3 to 4 events per month. However, during the study period, an increase in the occurrence of these wind events was observed, reaching between 7 and 8 events per month (Fig. 28).

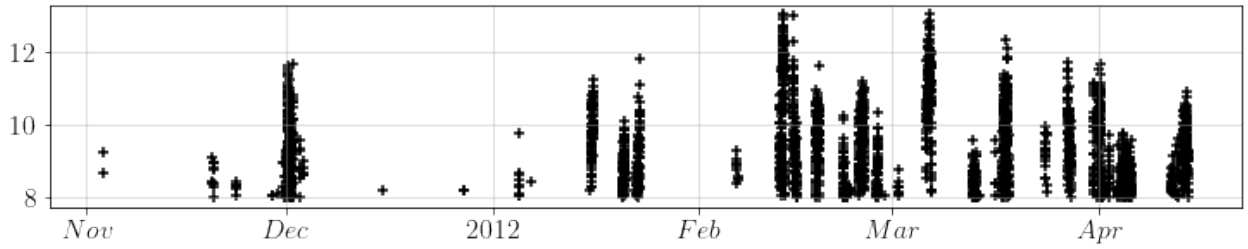

Figure 28: Occurrence of strong wind events in Pescadero estuary.

Sporadic abrupt changes in density along the water column in different locations were apparent during the periods of the closed state. These sudden changes indicate that they were not caused by gradual processes, but rather resulted from sporadic events that are attributed to the effects of wind stress present at the same time as the density changes. After these events, density did not return to its original values from before the event so mixing was present in the three studied locations.

Fig. 25 is showing density profiles in the studied locations before (in red) and after (in cyan) a big wind event, showing a difference in the density values, especially in the bottom where there is a decrease in density. Buoyancy frequency showed a decrease after the wind event meaning a change in stratification, same as the potential energy anomaly in Fig. 21. Also, in Fig. 23 $\Delta\rho/\Delta z$ is showing a decrease in stratification between before and after big wind events, only observing this abrupt change twice, with one time during each closed state period.

We chose to obtain a range of values for the Wedderburn number as we did not know the exact placement of the pycnocline. Due to the constant freshwater inflow, the stratification of the estuary is changing over time, which means the surface layer is also changing its thickness. The range limits of W were obtained as a function that depends directly on the water level. We assumed that at W=1 the density interface, in theory, reaches the upwind surface, so if the full range of W goes lower than that value we will consider it a full upwelling. During a full upwelling, if we consider a linear tilt, the lower limit reaches the surface, different from partial upwelling, where just the upper limit reaches the surface. The main difference between both events of upwelling is that the full one is changing the density structure and the other one is not. We can observe this in Fig. 21 where the potential energy anomaly after the partial upwelling events is not changing. During the upwelling events, there is the presence of baroclinic pressure gradients which increase with a lower W, so during the partial upwelling events, the gradients are not enough to mix the water column and change the stratification structure.

There were present surface fluctuations during the wind events, which are noticeable in the wavelet analysis in Fig. 26. Also, there is a small relation between wind and depth density frequencies (Fig. 27) around a period of 200 min.

6.4 Wind-driven circulation

During and after wind events there were observed circulation processes that are indicating how the layers of the estuary behave. We already noticed that the main driver of changes in velocity in the estuary is wind stress. In Fig. 29 we observed with more detail the circulation occurring around the first wind event of the second period. We observed that the estuary had some circulation occurring before the event, when there is no wind stress, due to the constant freshwater inflow that is present in Pescadero. This velocity is positive (streamflow direction) and is at the superior layer detected by the ADCP. Also, before the wind event, with $\tau_w = 0$, there was a negative velocity at the top of the range occurring at the same time as a detected wave overtopping event, meaning that the waves were creating a small circulation in the surface of the estuary that was overlapping the discharge velocity.

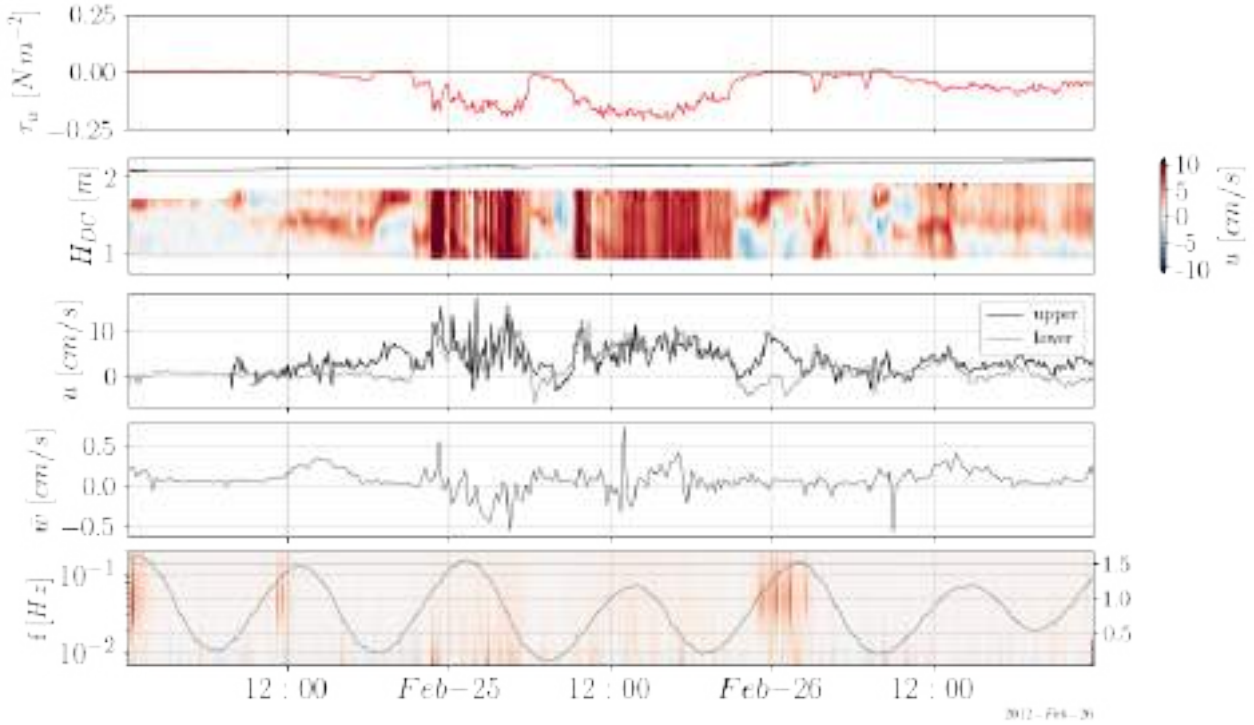

Figure 29: Time-series of wind stress (τ_w), along-estuary velocity in the water column, along-estuary velocity in the upper and lower layers of the ADCP range, and depth wavelet frequency analysis at DC and tidal height in San Francisco (gray).

During the wind event, we observed an increase in velocity in the positive direction, while the wind stress is negative. The literature says that a stratified waterbody that is subjected to surface stress has its surface layer circulating with the same direction of the wind with a set-up of the free surface at the leeward zone, depressing the pycnocline and resulting in set-down at the wind leeward shore and circulation of the lower layer in the opposite direction of the wind (Katopodes, 2019). Despite the last statement we observed in Fig. 29 the velocity during a wind event is in the opposite direction of the wind. This is due to the range of available data from the ADCP, which starts measuring at 0.91 m and doesn't work near the surface, not showing the surface layer circulation and skipping the part where the velocity is in the same direction as the wind. Also, when the wind blows, the upper layer moves towards the surface and upstream moving away

from the detected range (Fig. 30) making the upper layer thinner at the DC location.

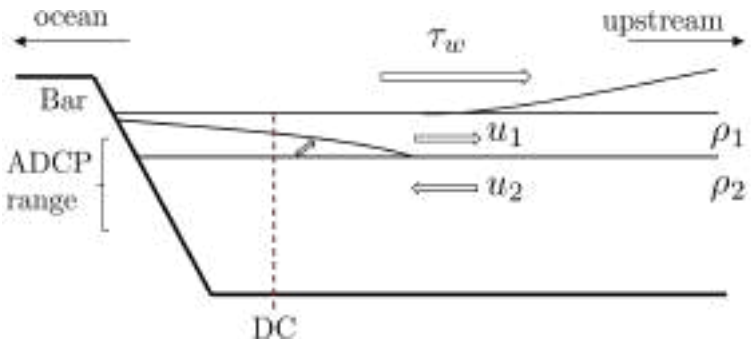

Figure 30: Scheme of the pycnocline tilt in an idealized estuary with the detected ADCP range in Pescadero.

Following the relaxation of the winds, the baroclinic pressure returns the estuary to its original state generating currents which are present mostly at the lower layers of the ADCP range (Fig. 29). We observed negative velocities after the first relaxation between the two wind increases. First, negative velocities were present at the lower part, representing the return of the middle layer to its equilibrium position, while at the top velocities were positive, maybe showing the surface layer dynamics. After less than two hours there was a flip on the dynamics, at the upper part positive and the lower negative, meaning probably a seiche in the estuary.

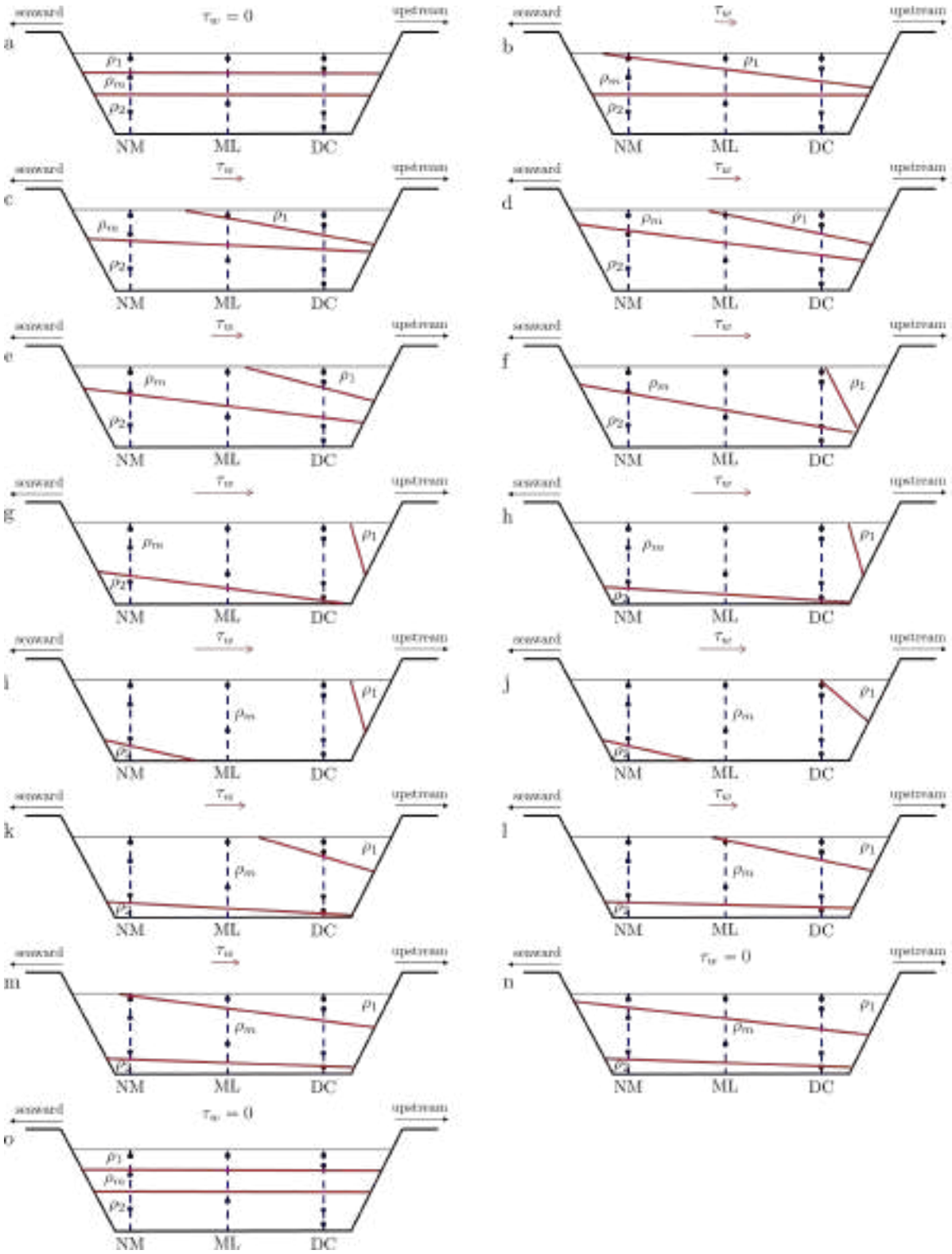

Figure 31: Movements of the density layers in Pescadero during the first wind event of the first period. The plots were constructed using the information given by the CTD.

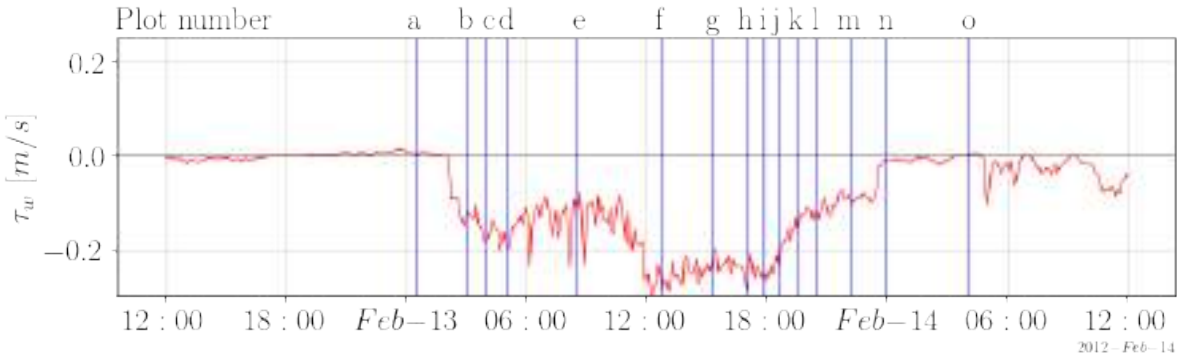

Figure 32: Wind event that was plotted in Fig. 31 with the instants of each plot.

The response to strong and sustained wind stress in a closed state bar-built estuary starts with a setup of the surface and a change in the pressure gradient. This will cause the pycnocline to tilt upwards at the upwind end of the estuary leading sometimes the bottom layers to rise to the surface. The reduction or end of this wind forcing releases the pycnocline from its tilted position and return to horizontal.

After the second increase, we noticed a similar dynamic to after the first increase, but we didn't observe the flip happen. We observed that at the same time there was a wave overtopping event that probably affected the recirculation, but as it did not cause the same effect as before of negative velocities at the top its possible that it is not affecting the velocities with the same magnitude or it is overlapping the velocities of the relaxation changing its behavior. Another reason for the flip not happening is that the oscillation hadn't enough amplitude, so the seiche didn't happen.

Also, we studied the first wind event of the first period using the densities at locations NM, ML, and DC. In Fig. 31 we plotted the behavior of the layers according to the densities at different instants of time shown at Fig. 32. The sensors' positions were put in the horizontal center of the estuary and had a distance proportional to reality in the vertical for an easier estimation of the layers with the available information. During the wind event, the surface layer is moving landward due to the wind stress going in that direction, not being shown by any sensor at the biggest wind stress. The middle layer was occupying the water column for all the sensors during the peak of the wind event. The lower layer had an uncertain movement, but we drew it as the sensors were showing it, going in the same direction as the middle layer, not having the behavior of a third layer.

6.5 Freshwater input

The density time-series were showing a density decrease in time, especially at the bottom layer in NM and ML (Fig. 20), in DC we also observed a decrease but not in the deepest layer, in which we observed a light increase of density in the first period. The density decrease in time indicates a constant freshwater input. The parameter $\Delta\rho/\Delta z$ is also slowly changing in time, a fact that is not observable in Fig. 23, but what is clear is the change between before and after a wind event that is decreasing over time, showing that wind stress is affecting each time less the estuarine structure. The last statement is also noticeable in the Wedderburn number (Fig. 22) where we observe in the last wind events W barely gets close to the threshold.

The destratification of the estuary could be a result of the freshwater constant input that is changing the density structure continuously in time. Also, it could be a result of the mixing that triggers the discharge increase

during storm events, due to water's faster entrance to the estuary, which can induce interfacial instability (Katopodes, 2019). The discharge increase is only reflected in the estuary at the surface (Fig. 19) and is not very clear in the density, especially as it happens at the same time as a wind event in the first period and a wave overtopping event in the second period. It is possible that the rapid increase in the incoming flow generate mixing, although there is not enough evidence to say that this is happening.

Like we said before, the two registered freshwater inflow increases happened with other events at the same time, the first one during a wind event and the other while there was wave overtopping. That is why we cannot attribute the changes observed in $\hat{H}$, dh/dt or $\Delta\hat{H}/\Delta x$ exclusively to discharge increase (Fig. 19). In Fig. 33 we observe discharge versus the water level and the level change over time. The first one had a strong correlation until Q started decreasing while H_{DC} still increase. The second plot also has some correlation, but we observe dh/dt is not increasing constant, so Q did not affect constantly the same at the water level increase rate, but still, there is a strong relationship between them.

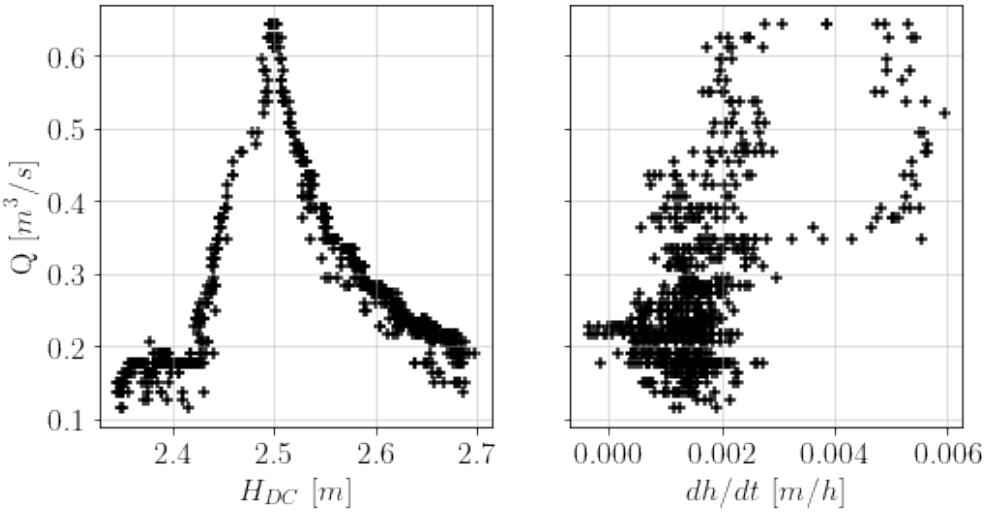

Figure 33: Discharge versus estuary height and discharge versus the height change in a 10-hour-frame for the period between 11 Feb. and 20 Feb..

Fig. 34 is showing the second discharge increase that happened at the same time as a wave overtopping event. We observed surface fluctuations in $\hat{H}$ while it was increasing and ϕ was increasing also, showing that Pescadero is stratifying instead of destratifying as was thought. When Q reached its highest value, it began to decrease and then became constant, while ϕ kept increasing until the wind event when momentarily reached lower values. When the wind stopped ϕ did not reach the same value that before showing the wind event reduced stratification.

The freshwater inflow is affecting stratification in the medium term and not in short term, not causing mixing when it increases, different from wind stress. Discharge is affecting the estuary by constantly and slowly reducing density.

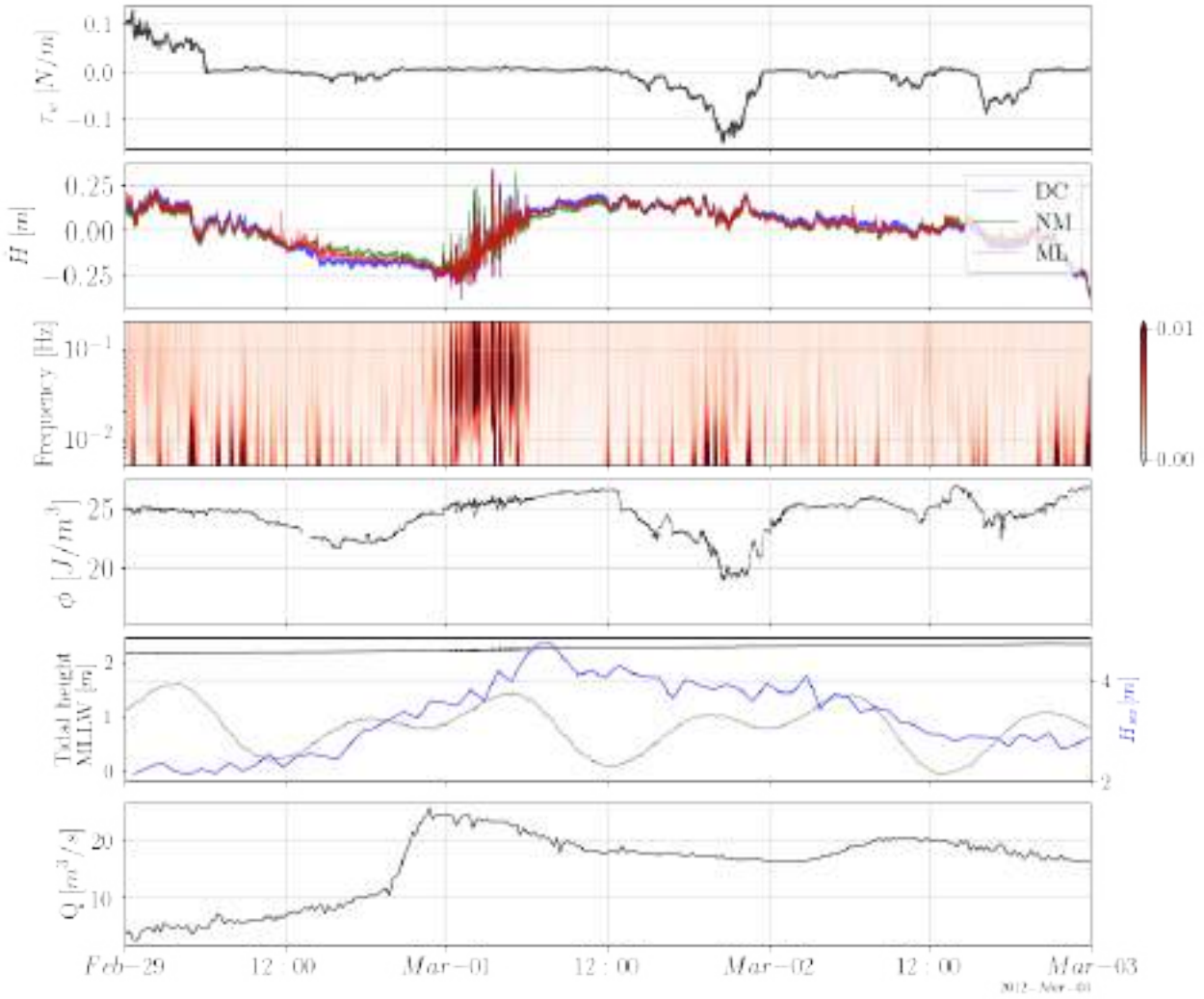

Figure 34: Time-series of wind stress (τ_w), standardized depth ($\hat{H}$) in DC, NM, and ML locations, depth wavelet frequency analysis at DC, the potential energy anomaly (ϕ), significant wave height in Halfmoon Bay (blue), and tidal height in San Francisco (gray), and freshwater discharge (Q).

6.6 Wave overtopping

Wave overtopping is an event that happens during high tide and relatively high significant wave height, but also can depend on the wave period or the wave direction. To determine the factors involved in this process Fig. 35 illustrates the tide level with significant wave height, dominant wave period, and dominant wave period direction as the estuary level rises. We noticed that two events happened with a significant wave height between 4 and 6 m and the others between 2 and 4 m. For the dominant wave period, we didn't observe a clear pattern, but the direction of the dominant period showed the events occurred between 300^o and 325^o.

As we already mentioned wave overtopping causes changes in surface velocities, which led us to believe that there would be mixing in the estuary during these events due to the turbulent entry of the waves over the sand bar. However, we couldn't find any evidence of it causing destratification or decrease of the ϕ in Fig. 34,

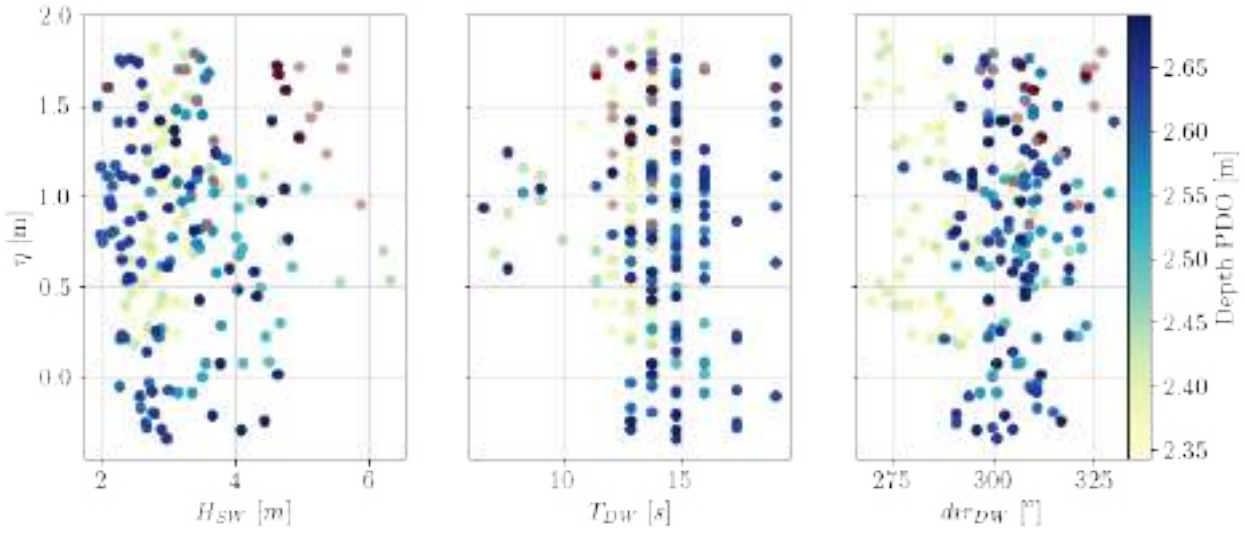

Figure 35: Tide level (η) versus significant wave height (H_{SW}), dominant wave period (T_{DW}), and dominant wave period direction (dir_{DW}) with the water level of Pescadero (Depth PDO) in colors, during the period between 11 Feb. and 20 Feb.. Four wave overtopping events were selected as the most prominent of the period and were marked in the plot with reddish stars.

probably because it wasn't an event big enough for the water level.

We observed a slow increase in density at the bottom layer of DC, which does not follow the same pattern of density decrease that the other locations had. In Fig. 36 there is a close-up of DC bottom density during the first period. First, we noticed that on 14 February there is an important wave overtopping event during which there is a negative spike in ρ_{DC}. After that, density started increasing but did not recover its value from before the spike. This could mean there was mixing due to the action of the waves, but as at the same time, there was a Q increase we cannot attribute any driver in specific. It could be the action of both causing the spike.

After that, the wind would further reduce the density and, later, it would progressively increase. During that increase, we observed a smaller decrease of density during a wind event and another during a wave overtopping event on 17 Feb. (Fig. 36). Consequently there is mixing due to the turbulent inflow of waves into the estuary that affects the deeper layer.

Also, the saline water inflow from the wave overtopping events could be causing the increase in density at the bottom of DC. The baroclinic effect could be making the saltwater set at the bottom slowly after the waves, but also it is possible that there is not enough saline water to change salinity and a baroclinic effect alone is acting in Pescadero.

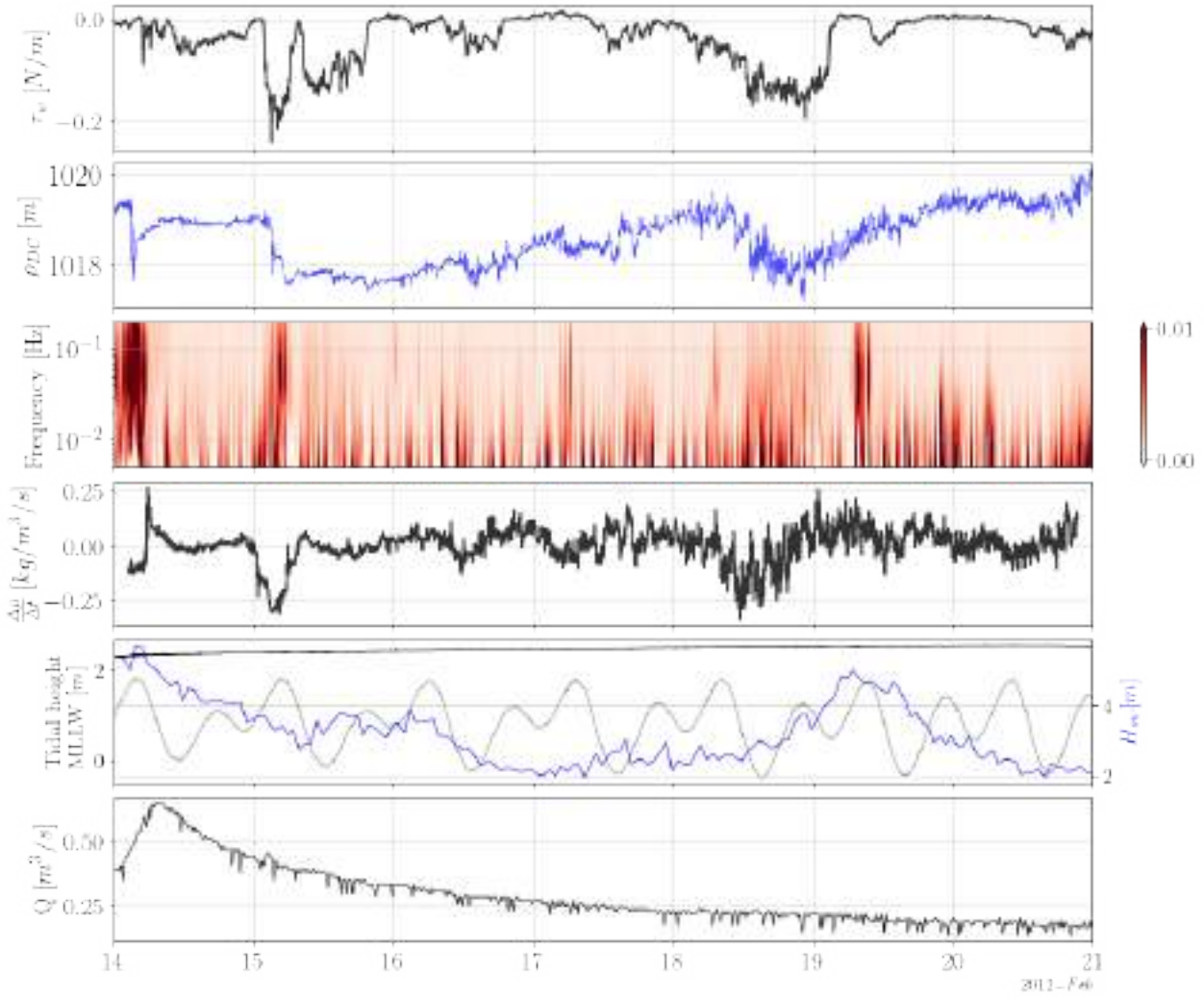

Figure 36: Time-series of wind stress (τ_w), bottom density in DC location (ρ_{DC}), depth wavelet frequency analysis at DC, the change of density in a 10-hour time frame ($\Delta\rho/\Delta t$), significant wave height in Halfmoon Bay (blue), tidal height in San Francisco (gray), and Pescadero estuary water level (black) in MLLW datum, and freshwater discharge (Q).

7 Conclusions

The analyzes carried out showed how wind, freshwater inflow, and tide are influencing the stratification and dynamics of the Pescadero estuary. To quantify these effects the potential energy anomaly was applied (ϕ). We could notice that the constant discharge from Pescadero and Butano creek is changing water level and stratification in the estuary, as observed in Fig. 21, where is noticeable that each wind event is affecting each time less the estuarine structure, due to the increase of the upper layer thickness. Also, ϕ decreased after each wind event showing mixing in the water column. The effects of both external factors, wind and flow, counteract each other, one contributing to stratification and the other causing mixing in the estuary, however the biggest change in ϕ was due to a wind event, showing that it is the main driver of stratification changes.

Wind force caused a big impact in the estuarine dynamics, and was demonstrated to cause changes in density layers during and after wind influence (Fig. 25). It is shown that wind stress moved the layers causing upwelling during the wind events and, when stopped, stratified the water column but with different density changes between the surface and the bottom, demonstrating there was mixing present during the wind event. W, ϕ, and N^2 demonstrate the effect of the wind in the watercolumn during the two study periods and how mixing is present (Figs. 21, 22, 25). The intensity of upwelling significantly hinges on the duration of winds in relation to the baroclinic setup period, encompassing scenarios where wind duration surpasses the setup time by several multiples (Roberts et al., 2021). The observed patterns during the wind events are consistent with the theory.

There was saltwater inflow caused by wave overtopping in the estuary, but it was not big enough to change stratification in long term as previously thought. Anyways there was a slow increase in the deeper layer of DC location that could be driven by wave overtopping. We also observed some increases in the stratification on the other layers but were only temporary and small. No evidence was found that the wave overtopping was causing reduction of the potential energy anomaly (Fig. 34).

The estuarine circulation dynamics were effectively captured through the analysis of velocity profiles in our studies. Notably, the presence of circulation was discernible even in the absence of wind stress, as illustrated in Fig. 29. This circulation pattern, marked by positive velocities at the surface (indicating the direction of the current) and negative velocities in the lower layers, aligns with expectations for the freshwater inflow entering the estuary. Additionally, observations during instances of wave overtopping events showed negative velocities at the upper range coincided with the detected wave overtopping, signifying that the waves briefly induced a circulation within the estuary. This phenomenon overlapped with the discharge velocity, shedding light on the interactions between wave dynamics and estuarine circulation.

The circulation caused by the wind stress was not fully captured by the velocity profiles due to the instrumental range of the ADCP. Fig. 330 shows the dynamics of the estuary during a wind event, which is consistent with what was expected for this study. In addition, it is observed that in Fig. 29 and in Fig. 25 when the first wind event ends, between 6:00 and 11:00 on 25 Feb., the velocities are reversed, which is attributable to the relaxation of the estuary after the wind event. Between this period no high tide was detected, which reduces the possibility of waves entering the estuary, and their presence was not observed at the surface in the wavelet analysis.

The wind affected the behavior of the estuarine water level (Fig. 26). During the wind event, an upward tilt was observed (higher water level at DC), which was reversed during wind relaxation (higher water level at ML), generating an oscillation with period of 11.75 ± 2.72 min. Spectral analysis (Fig. 27) showed that the wind oscillation frequencies are indeed reflected in the surface fluctuations, between the frequencies $5 * 10^{-5}$ and $1 * 10^{-4}$. The flow rate is related to the water level in the estuary as shown in Fig. 33, but this was not observed to be influencing the fluctuations at the surface during the recorded flow increases. In Pescadero, it can be observed that there is wave overtopping, and that this causes fluctuations on the surface that can be observed in the wavelet analysis in the range $2 * 10^{-2}$ to $2 * 10^{-1}$ (Fig. 36). In addition, the wave overtopping did not cause an increase in water level.

In summary, wind stress significantly contributes to mixing the water column through upwelling in a small and highly stratified estuary. The density structure changes can result from a variety of processes. Which of these processes are relevant in a specific estuary depends on its morphology, its salinity, and also its stratification. The stratification and other conditions such as the area and depth at the estuary affect the occurrence of

upwelling and mixing events. In the same way, changes in the wind stress events' magnitude and duration or in the estuarine morphologic conditions, including changes in water level, will have consequences for stratification mainly because of a change in upwelling occurrence. The results of this work could be applied to other small estuaries with seasonal or permanent closures like coastal lagoons.

References

Avalos Cueva, D., Monzón, C. O., Filonov, A., Tereshchenko, I., Limón Covarrubias, P., and Galaviz González, J. R. (2019). Natural frequencies of seiches in Lake Chapala. *Scientific Reports*, 9(1):1–11.

Bastidas, L., Piedrahita, R., and Llanos-Rivera, A. (2021). A comparison of upwelling systems: A review of physical processes and ecosystem effects. *Progress in Oceanography*, 191:102475.

Behrens, D. K., Bombardelli, F. A., and Largier, J. L. (2016). Landward propagation of saline waters following closure of a bar-built estuary: Russian River (California, USA). *Estuaries and Coasts*, 39(3):621–638.

Behrens, D. K., Bombardelli, F. A., Largier, J. L., and Twohy, E. (2013). Episodic closure of the tidal inlet at the mouth of the Russian River—A small bar-built estuary in California. *Geomorphology*, 189:66–80.

Clark, R. and O'Connor, K. (2019). A systematic survey of bar-built estuaries along the California coast. *Estuarine, Coastal and Shelf Science*, 226:106285.

Clarke, D. W., Boyle, J. F., Lario, J., and Plater, A. J. (2014). Meso-scale barrier estuary disturbance, response and recovery behaviour: Evidence of system equilibrium and resilience from high-resolution particle size analysis. *The Holocene*, 24(3):357–369.

Coman, M. A. and Wells, M. G. (2012). Temperature variability in the nearshore benthic boundary layer of Lake Opeongo is due to wind-driven upwelling events. *Canadian Journal of Fisheries and Aquatic Sciences*, 69(2):282–296.

Cousins, M., Stacey, M. T., and Drake, J. L. (2010). Effects of seasonal stratification on turbulent mixing in a hypereutrophic coastal lagoon. *Limnology and Oceanography*, 55(1):172–186.

Curry, R., Houghton, R., Kidwell, T., and Tang, P. (1985). Pescadero marsh management: A plan for persistence and productivity.

de la Fuente, A., Meruane, C., Contreras, M., Ulloa, H., and Niño, Y. (2010). Strong vertical mixing of deep water of a stratified reservoir during the Maule earthquake, central Chile (Mw 8.8). *Geophysical Research Letters*, 37(24).

de la Fuente, A., Shimizu, K., Imberger, J., and Nino, Y. (2008). The evolution of internal waves in a rotating, stratified, circular basin and the influence of weakly nonlinear and nonhydrostatic accelerations. *Limnology and Oceanography*, 53(6):2738–2748.

Dussaillant, A., Galdames, P., and Sun, C.-L. (2009). Water level fluctuations in a coastal lagoon: El yali ramsar wetland, chile. *Desalination*, 246(1-3):202–214.

Gale, E., Pattiaratchi, C., and Ranasinghe, R. (2006). Vertical mixing processes in intermittently closed and open lakes and lagoons, and the dissolved oxygen response. *Estuarine, Coastal and Shelf Science*, 69(1-2):205–216.

Gupta, M., Williams, R. G., Lauderdale, J. M., Jahn, O., Hill, C., Dutkiewicz, S., and Follows, M. J. (2022). A nutrient relay sustains subtropical ocean productivity. *Proceedings of the National Academy of Sciences*, 119(41):e2206504119.

Hewitt, J. E., Ellis, J. I., and Thrush, S. F. (2016). Multiple stressors, nonlinear effects and the implications of climate change impacts on marine coastal ecosystems. *Global change biology*, 22(8):2665–2675.

Hoeksema, S. D., Chuwen, B. M., Tweedley, J. R., and Potter, I. C. (2018). Factors influencing marked variations in the frequency and timing of bar breaching and salinity and oxygen regimes among normally-closed estuaries. *Estuarine, Coastal and Shelf Science*, 208:205–218.

Holt, J., Wakelin, S., Lowe, J., and Tinker, J. (2010). The potential impacts of climate change on the hydrography of the northwest european continental shelf. *Progress in Oceanography*, 86(3-4):361–379.

Huber, E. R. and Carlson, S. M. (2020). Environmental correlates of fine-scale juvenile steelhead trout (oncorhynchus mykiss) habitat use and movement patterns in an intermittent estuary during drought. *Environmental Biology of Fishes*, 103(5):509–529.

Human, L. R. D., Snow, G. C., and Adams, J. B. (2016). Responses in a temporarily open/closed estuary to natural and artificial mouth breaching. *South African Journal of Botany*, 107:39–48.

Imam, Y. E., Laval, B., Pieters, R., and Lawrence, G. (2013). The strongly damped baroclinic response to wind in a multibasin reservoir. *Limnology and oceanography*, 58(4):1243–1258.

Imberger, J. and Hamblin, P. F. (1982). Dynamics of lakes, reservoirs, and cooling ponds. *Annual Review of Fluid Mechanics*, 14(1):153–187.

Jayaweera, H., Lowe, R., Zhang, H., and Pattiaratchi, C. (2019). Turbulent mixing across the pycnocline under varying wind and buoyancy forcing: Observations from a coastal lagoon. *Journal of Geophysical Research: Oceans*, 124(8):6035–6054.

Jones, P. D., New, M., Parker, D. E., Martin, S., and Rigor, I. G. (1999). Surface air temperature and its changes over the past 150 years. *Reviews of Geophysics*, 37(2):173–199.

Katopodes, N. D. (2019). Chapter 11 - stratified flow. In Katopodes, N. D., editor, *Free-Surface Flow*, pages 780–839. Butterworth-Heinemann.

Kelly, S., de Eyto, E., Dillane, M., Poole, R., Brett, G., and White, M. (2018). Hydrographic maintenance of deep anoxia in a tidally influenced saline lagoon. *Marine and Freshwater Research*, 69(3):432–445.

Kundu, P. K., Cohen, I. M., and Dowling, D. R. (2015). *Fluid Mechanics*. Academic press.

Large, W. and Pond, S. (1981). Open ocean momentum flux measurements in moderate to strong winds. *Journal of Physical Oceanography*, 11(3):324–336.

Largier, J. (2021). Hydrological responses to closure in Californian estuaries. Coastal & Marine Sciences Institute, University of California Davis, Global Forum on Intermittent Estuaries. `https://www.youtube.com/watch?v=HXWZNu1KYMQ&t=140s`.

Largier, J., Aiello, I., Jacobs, D., Lacy, J., Pallud, C., Stacey, M., Carlson, S., Huber, E., and Bowles, C. (2015). Report of pescadero lagoon science panel. `https://repository.library.noaa.gov/view/noaa/40845/noaa_40845_DS1.pdf`.

Laudier, N. A., Thornton, E. B., and MacMahan, J. (2011). Measured and modeled wave overtopping on a natural beach. *Coastal Engineering*, 58(9):815–825.

Laval, B. E., Morrison, J., Potts, D. J., Carmack, E. C., Vagle, S., James, C., McLaughlin, F. A., and Foreman, M. (2008). Wind-driven summertime upwelling in a fjord-type lake and its impact on downstream river conditions: Quesnel Lake and River, British Columbia, Canada. *Journal of Great Lakes Research*, 34(1):189–203.

Lee, G., Gommers, R., Waselewski, F., Wohlfahrt, K., and O'Leary, A. (2019). Pywavelets: A python package for wavelet analysis. *Journal of Open Source Software*, 4(36):1237.

MacIntyre, S., Rueda, F. J., and S'anchez-Garc'ıa, E. (2010). Ecosystem responses to coastal upwelling: A comparison of four major eastern boundary upwelling systems. *Journal of Marine Systems*, 83(3-4):244–255.

Marti-Cardona, B., Steissberg, T., Schladow, S. G., and Hook, S. (2008). Relating fish kills to upwellings and wind patterns in the salton sea. In *The Salton Sea Centennial Symposium*, pages 85–95. Springer.

Martínez, M. L., Intralawan, A., Vázquez, G., Pérez-Maqueo, O., Sutton, P., and Landgrave, R. (2007). The coasts of our world: Ecological, economic and social importance. *Ecological Economics*, 63(2-3):254–272.

McSweeney, S., Kennedy, D., Rutherfurd, I., and Stout, J. (2017). Intermittently closed/open lakes and lagoons: Their global distribution and boundary conditions. *Geomorphology*, 292:142–152.

Monismith, S. G. (1985). Wind-forced motions in stratified lakes and their effect on mixed-layer shear. *Limnology and oceanography*, 30(4):771–783.

Monismith, S. G., Kim, J. H., and Lacy, J. R. (2006a). Turbulent processes in lakes and oceans. *Annual Review of Fluid Mechanics*, 38(1):97–122.

Monismith, S. G., Kimmerer, W. J., and Burau, J. R. (2006b). Vertical mixing and coastal upwelling in stratified, tidally mixed estuaries. *Estuaries and Coasts*, 29(2):347–361.

Neumann, B., Vafeidis, A. T., Zimmermann, J., and Nicholls, R. J. (2015). Future coastal population growth and exposure to sea-level rise and coastal flooding-a global assessment. *PloS one*, 10(3):e0118571.

Nidheesh, A., Gandhimathi, R., and Suguna, J. (2018). Stratification dynamics in a freshwater reservoir under changing thermal regime. *Journal of Hydro-environment Research*, 19:9–19.

Nunes, M. and Adams, J. (2014). Responses of primary producers to mouth closure in the temporarily open/closed Great Brak Estuary in the warm-temperate region of South Africa. *African Journal of Aquatic Science*, 39(4):387–394.

Omstedt, A., Pettersen, C., Rodhe, J., and Winsor, P. (2004). Baltic Sea climate: 200 yr of data on air temperature, sea level variation, ice cover, and atmospheric circulation. *Climate Research*, 25(3):205–216.

Patterson, J., Hamblin, P., and Imberger, J. (1984). Classification and dynamic simulation of the vertical density structure of lakes 1. *Limnology and oceanography*, 29(4):845–861.

Paugam, C., Sous, D., Rey, V., Meulé, S., Faure, V., Boutron, O., Luna-Laurent, E., and Migne, E. (2021). Wind tides and surface friction coefficient in semi-enclosed shallow lagoons. *Estuarine, Coastal and Shelf Science*, 257:107406.

Peeters, F. and Kipfer, R. (2009). Currents in stratified water bodies 1: Density-driven flows. In Likens, G. E., editor, *Encyclopedia of Inland Waters*, pages 530–538. Academic Press, Oxford.

Ranasinghe, R. and Pattiaratchi, C. (1999). The seasonal closure of tidal inlets: Wilson Inlet—a case study. *Coastal Engineering*, 37(1):37–56.

Ranasinghe, R. and Pattiaratchi, C. (2003). The seasonal closure of tidal inlets: causes and effects. *Coastal engineering journal*, 45(04):601–627.

Read, J. S., Hamilton, D. P., Jones, I. D., Muraoka, K., Winslow, L. A., Kroiss, R., Wu, C. H., and Gaiser, E. (2011). Derivation of lake mixing and stratification indices from high-resolution lake buoy data. *Environmental Modelling & Software*, 26(11):1325–1336.

Richards, C. M., Moal, O., and Pallud, C. (2018). Changes in water quality following opening and closure of a bar-built estuary (pescadero, california). *Marine Chemistry*, 198:10–27.

Roberts, D. C., Egan, G. C., Forrest, A. L., Largier, J. L., Bombardelli, F. A., Laval, B. E., Monismith, S. G., and Schladow, G. (2021). The setup and relaxation of spring upwelling in a deep, rotationally influenced lake. *Limnology and Oceanography*, 66(4):1168–1189.

Roquet, F., Madec, G., McDougall, T. J., and Barker, P. M. (2015). Accurate polynomial expressions for the density and specific volume of seawater using the teos-10 standard. *Ocean Modelling*, 90:29–43.

Schernewski, G. (2002). *Baltic Coastal Ecosystems: Structure, Function and Coastal Zone Management*. Springer Science & Business Media.

Schmidtko, S., Stramma, L., and Visbeck, M. (2017). Decline in global oceanic oxygen content during the past five decades. *Nature*, 542(7641):335–339.

Shintani, T., de la Fuente, A., de la Fuente, A., Niño, Y., and Imberger, J. (2010). Generalizations of the Wedderburn number: Parameterizing upwelling in stratified lakes. *Limnology and Oceanography*, 55(3):1377–1389.

Simpson, J., Sharples, J., and Rippeth, T. (1991). A prescriptive model of stratification induced by freshwater runoff. *Estuarine, Coastal and Shelf Science*, 33(1):23–35.

Simpson, J. H., Brown, J., Matthews, J., and Allen, G. (1985). Tidal straining, density currents, and stirring in the control of estuarine stratification. *Estuaries*, 13:125–132.

Sloan, R. M. (2006). Ecological investigations of a fish kill in Pescadero Lagoon, California. 3032. Master's Theses.

Stevens, C. and Imberger, J. (1996). The initial response of a stratified lake to a surface shear stress. *Journal of Fluid Mechanics*, 312:39–66.

Teledyne, R. I. (2008). Adcp coordinate transformation: Formulas and calculations.

Thorne, K. M., Buffington, K. J., Jones, S. F., and Largier, J. L. (2021). Wetlands in intermittently closed estuaries can build elevations to keep pace with sea-level rise. *Estuarine, Coastal and Shelf Science*, 257:107386.

Valerio, G., Pilotti, M., Marti, C. L., and rg Imberger, J. (2012). The structure of basin-scale internal waves in a stratified lake in response to lake bathymetry and wind spatial and temporal distribution: Lake Iseo, Italy. *Limnology and Oceanography*, 57(3):772–786.

Viaroli, P., Bartoli, M., Giordani, G., Naldi, M., Orfanidis, S., and Zaldivar, J. M. (2008). Community shifts, alternative stable states, biogeochemical controls and feedbacks in eutrophic coastal lagoons: a brief overview. *Aquatic Conservation: Marine and Freshwater Ecosystems*, 18(S1):S105–S117.

Welch, P. (1967). The use of fast Fourier transform for the estimation of power spectra: a method based on time averaging over short, modified periodograms. *IEEE Transactions on audio and electroacoustics*, 15(2):70–73.

Whitfield, A. and Bate, G. (2007). A review of information on temporarily open/closed estuaries in the warm and cool temperate biogeographic regions of South Africa, with particular emphasis on the influence of river flow on these systems. *Water Research Commission, Report*, 1581(1):07.

Whitfield, A. and Wooldridge, T. (1994). Changes in freshwater supplies to southern african estuaries: some theoretical and practical considerations. *OLSEN & OLSEN, FREDENSBORG, DENMARK.*, pages 41–50.

Williams, J. et al. (1990). Pescadero marsh natural preserve hydrologic enhancement plan. *Prepared for California Department of Parks and Recreation. Report no. 504, 31 August. Prepared by Phillip Williams and Associates, San Francisco, California*.

Williams, M. (2014). Hydrodynamics and salt dispersion in intermittently closed bar-built estuaries. *PhD Thesis*. UC Berkeley.

Williams, M. and Stacey, M. T. (2016). Tidally discontinuous ocean forcing in bar-built estuaries: The interaction of tides, infragravity motions, and frictional control. *Journal of Geophysical Research: Oceans*, 121(1):571–585.

Winckler, P., Aguirre, C., Farías, L., Contreras-López, M., and Masotti, Í. (2020). Evidence of climate-driven changes on atmospheric, hydrological, and oceanographic variables along the chilean coastal zone. *Climatic Change*, 163(2):633–652.

Winckler Grez, P., Aguirre, C., Farías, L., Contreras-López, M., and Masotti, Í. (2020). Evidence of climate-driven changes on atmospheric, hydrological, and oceanographic variables along the chilean coastal zone. *Climatic Change*, 163(2):633–652.

Woolway, R. I., Meinson, P., Nõges, P., Jones, I. D., and Laas, A. (2017). Atmospheric stilling leads to prolonged thermal stratification in a large shallow polymictic lake. *Climatic Change*, 141(4):759–773.

Wüest, A. and Lorke, A. (2003). Small-scale hydrodynamics in lakes. *Annual Review of fluid mechanics*, 35(1):373–412.

Xu, D., Hesser, T., and Mayer, T. (2017). Vertical exchange and interfacial layer dynamics in two-layered shallow estuaries. *Journal of Geophysical Research: Oceans*, 122(7):5506–5525.